

DOCKET

09-AFC-6

DATE JUN 16 2010

RECD. JUN 17 2010

June 16, 2010

Alan Solomon
Project Manager
California Energy Commission
1516 Ninth Street
Sacramento, CA 95814

RE: Blythe Solar Power Project, Docket No. 09-AFC-6

Computational Fluid Dynamics of an Air Cooled Condenser in a Convectively Unstable Boundary Layer

Dear Mr. Solomon:

Attached please find the following computational fluid dynamics modeling of an air cooled condenser in a convectively unstable boundary layer

If you have any questions on this submittal, please feel free to contact me directly.

Sincerely,



Alice Harron
Senior Director, Development



Environment

Prepared for:
Palo Verde Solar I, LLC
Berkeley, CA

Prepared by:
AECOM
Camarillo, CA
60139695-6300
June

Computational Fluid Dynamics Modeling of an Air Cooled Condenser in a Convectively Unstable Boundary Layer



Environment

Prepared for:
Palo Verde Solar I, LLC
Berkeley, CA

Prepared by:
AECOM
Camarillo, CA
60139695-6300
June

Computational Fluid Dynamics Modeling of an Air Cooled Condenser in a Convectively Unstable Boundary Layer

Authors:

Gary Moore
Serkan Mahmutoglu
Howard Balentine

Contents

Executive Summary.....	1-1
1.0 Introduction.....	1-1
1.1 Statement of the Problem.....	1-2
1.2 Approach.....	1-3
2.0 Development of a Conceptual Model.....	2-1
2.1 The Convectively Unstable Boundary Layer.....	2-1
2.2 Plume Rise Analysis.....	2-3
2.2.1 Model Selection.....	2-5
3.0 Description of the Modeling Environment.....	3-1
3.1 Geographical Data.....	3-1
3.2 Meteorological Characteristics.....	3-5
3.2.1 Surface Data Analysis.....	3-5
3.2.2 Upper Air Analysis.....	3-5
3.3 Surface Calm Conditions.....	3-9
4.0 CFD Model Input Preparation.....	4-1
4.1 Physical Layout of the ACC and Modeling Domain.....	4-1
4.2 Development and Application of Boundary and Initial conditions.....	4-2
4.2.1 Surface Material Characteristics.....	4-2
4.2.2 Input Boundary and Initial Conditions.....	4-3
4.3 Determination of the Modeling Grid.....	4-7
5.0 WIND 3-D Application and Analysis.....	5-1
5.1 Description of Simulations.....	5-1
5.2 Visualization of Simulation Results.....	5-2
5.2.1 Idealized Simulations.....	5-2
5.2.2 Final Simulation (Phase 3).....	5-2
5.2.3 Impact on Flight Characteristics.....	5-3
6.0 References.....	6-1

List of Attachments

Attachment 1. Inflow Boundary Layer Parameter Profiles

List of Tables

Table 2-1. Summary of Values.	2-1
Table 2-2. Physical characteristics of the ACC proposed for the BSPP	2-3
Table 5-1. A summary of CFD simulations	5-1

List of Figures

Figure 1-1. Current and Proposed Traffic Patterns at Blythe Airport Representing Approximately 80 Percent of Average Traffic.	1-2
Figure 2-1. Qualitative illustration of normalized plume trajectories (plume shape) in the unstable boundary layer (courtesy of Csanady , 1973)	2-2
Figure 2-2. Schematic diagram of a typical ACC cell showing axial fan (green), fan shroud (gray), supporting structure (dark gray), steam header (red), and heat transfer tubes (blue).....	2-4
Figure 3-1. A satellite image of the proposed ACC site. The northern tip of the Blythe Municipal Airport is shown at the very bottom adjacent to old irrigation circles.....	3-2
Figure 3-2. A plot of the terrain and land cover category within 2 km of the proposed ACC	3-3
Figure 3-3. An image plot overlaid by the FAA exclusion zones and the location of the proposed ACC3-4	
Figure 3-4. Wind rose of the ASOS (10 m hourly) winds at the Blythe Municipal Airport (BLH) during the hours 0900-1800 LST	3-7
Figure 3-5. Vertical profiles of potential temperature observed from mid-day rawinsondes released at Edwards AFB during June-August with wind speeds less than 1.0 m/s in the first reporting level (1990-2010).....	3-8
Figure 3-6. Vertical profiles of wind speed observed from midday rawinsondes released at Edwards AFB during June-August with wind speeds less than 1.0 m/s in the first reporting level (1990-2010)	3-9
Figure 3-7. The temperature (°C) just above and below the surface of sparsely vegetated sandy plains in the Sonoran Desert, averaged for July and August 1956. The dashed and dotted lines define the time of the temperature maximum and minimum at each height or depth. Note the non-uniform isotherm interval. (Adapted from Dodd and McPhilimy, 1959.).....	3-11
Figure 4-1. A plot of the three sub regions, desert, solar collector array, and ACC.	4-4
Figure 4-2. A picture showing a parabolic mirror solar array at the Kramer Junction SEGS plant	4-5
Figure 4-3. X-Z side view of the modeling domain mesh used in the present study.	4-7

Figure 4-4. Magnified X-Z side view of the modeling domain mesh used in the present study centered on the ACC. 4-8

Figure 5-1. A snapshot of the X-Z cross section of upwards directed (positive) vertical wind speed at 2000 seconds into the simulation in a convectively unstable boundary layer resulting in a looping plume. The ACC is in the range (-39,39)..... 5-4

Figure 5-2. A vertical profile of minimum and maximum vertical wind speed found in each model layer (10 m layers)..... 5-5

Figure 5-3. An X-Z cross section snapshot showing the horizontal wind speed (m/s) in the immediate vicinity of the ACC at 2,000 seconds into the simulation. The ACC is in the range (-39,39)..... 5-6

Figure 5-4. An X-Z cross section snapshot showing the air density profile (kg/m³) in the immediate vicinity of the ACC at 2,000 seconds into the simulation. The ACC is in the range (-39,39)..... 5-7

Figure 5-5. The profile of maximum change in aircraft pitch angle as a function of height above the ground experienced by an aircraft at 80 mph (35 m/s) due to the ACC thermal plume alone over a 5 second period and absent the influence of the boundary layer convective..... 5-8

Figure 5-6. The vertical profiles of g-force accelerations as a function of height above the ground experienced by an aircraft at 80 mph (35 m/s) due to the ACC thermal plume alone over a 5 second period and absent the influence of the boundary layer convective 5-9

Figure 5-7. The vertical profiles of the maximum change in bank angle as a function of height above the ground experienced by an aircraft at 80 mph (35 m/s) due to the ACC thermal plume alone over a 5 second period and absent the influence of the boundary layer convective..... 5-10

Executive Summary

The Blythe Solar Power Project (BSPP, or Project) is a 1,000 megawatt commercial solar thermal power generating facility proposed by Palo Verde Solar, Inc. (PVSI) for development in the relatively flat desert region west of Blythe, California. The Project is located just northwest of the Blythe Municipal Airport. Portions of the project site lie within the Airport Influence Area (AIA) as defined by the Riverside County Airport Land Use Commission (ALUC). The California Energy Commission and the RCALUC are concerned with the potential impact of thermal plumes from BSPP air cooled condensers (ACCs) on aircraft flight safety at the Blythe Airport. For the BSPP ACCs, the concern is that the thermal updrafts and turbulence associated with the fan-driven thermal plume coming off the ACC finned heat exchangers will interfere with aircraft stability at the Blythe Airport if an aircraft were to overfly a thermal plume. Four ACCs proposed for the BSPP, one for each of the four power blocks. None of the ACCs will be located within the Blythe Airport AIA but one will be close to the AIA boundary. To address CEC and RCALUC concerns, PVSI initiated a modeling study of the thermal plume from an ACC located in the desert environment. A companion study documents the results of a light aircraft flyover of a similar ACC at an operating power plant in a desert environment.

During operation, an ACC releases a large amount of thermal energy into the surface meteorological boundary layer above the ACC. Being warmer than the surrounding air, the release of thermal energy creates a thermal plume that can potentially cause turbulence above the ACC that could affect flight safety. However, any such thermal plume will be released into a desert environment that is subject to the natural occurrence of convective thermal plumes that result from the intense insolation that occurs in a desert location on a sunny day. At peak loads at midday, the thermal plume will interact with the convective thermals in the surrounding desert environment which will dramatically affect the rise and dissipation of the ACC thermal plume. Thus, an ACC has the potential to contribute additional turbulence to the already existing natural turbulence associated with convective thermals. It should be noted, however, that BSPP will only operate during the daytime when there is available sunlight. Consequently, the ACCs only have the potential to affect flight safety during daylight hours when they are operating.

A numerical modeling approach using computation fluid dynamic (CFD) modeling techniques was selected for this modeling study. Such models that numerically solve the Reynolds Averaged Navier-Stokes (RANS) equations have recently proven themselves, when applied properly, to be realistic predictors of turbulent flow. The FLOW-3D model was selected for the present analysis owing to its ability to rapidly generate an appropriate modeling mesh, and numerical efficiency to rapidly exercise a number of numerical tests. FLOW-3D also has both a user friendly interface as well as a sophisticated visualization system to view model predicted parameters as profiles, slices, surface, trajectories, vectors, etc.

Three modeling sub-regions were used in the model setup. The outer coarse domain represented the convectively unstable desert thermal internal boundary layer (TIBL) at equilibrium. The land use is unimproved, sandy desert. The middle region was composed of the solar mirror arrays. The innermost region was represented by a high resolution mesh consisting of a footprint describing the ACC fans and A-frame slotted/finned heat diffusers.

The modeling analysis assumed a convective unstable boundary layer with near calm winds at the surface and a wind speed of 2 m/s at 100 meters with a westerly wind flow (from the west). Boundary layer theory indicates that a true calm wind through a deep layer of a convective boundary layer is not a realistic occurrence. A multiple mesh grid was established over the ACC and surrounding solar

trough array, with dry sand and desert scrub land outside the solar array. Detailed assessment of the boundary layer and meteorological characteristics of the simulation were examined prior to settling on the final scenario modeled. The vertical total kinetic energy (TKE) profile was carefully established to produce a representative desert environment for the simulation.

The boundary layer for this simulation was represented by a super adiabatic lapse rate near the surface that gradually transforms into a unstable layer in the middle part of the modeling domain, and eventually transforms into a neutral layer at the top of the modeling domain. The focus of the analysis is on the vertical wind velocities in the first 500 m (1,640 ft) that can be expect to be generated under such convectively unstable conditions.

The results of the modeling of the vertical velocity above the ACC indicates that the peak upward vertical plume velocity in the ACC thermal plume 250 m (820 ft) and above is less than 2 m/s. There are no winds exceeding 4.3 m/ anywhere in the domain except within a few 10's of meters immediately above the ACC, a location where an aircraft would not fly. This analysis demonstrates that the potential vertical velocities produced by an ACC thermal plume to which an aircraft could be exposed if it were to inadvertently fly over an operating ACC are less than approximately half of the CEC significance criteria of 4.3 m/s.

The modeling also includes assessment of potential pitch, bank, and vertical acceleration of an aircraft. Based on a response time of 5 seconds to depart from level flight due to interaction with the thermal plume of the ACC, and as limited by the modeling spatial and temporal resolution, no hazardous pitch, bank or vertical accelerations are modeled to occur that would produce a flight safety issue with a general aviation aircraft flying through the ACC plume. In addition, the magnitude of such flight perturbations was less than that from the naturally occurring thermal convection in the convectively unstable boundary layer.

Based on this modeling analysis, we conclude that thermal plumes produced by an ACC operating at the BSPP will not pose a threat to flight stability of aircraft taking off, landing, or operating near the Blythe Airport or in the vicinity of the BSPP. In addition, the ACCs proposed at the BSPP are located such that they are well out of the existing and proposed landing pattern for aircraft operating the Blythe Airport

1.0 Introduction

The Blythe Solar Power Project (BSPP, or Project) is a 1,000 megawatt commercial solar thermal power generating facility proposed by Palo Verde Solar, Inc. (PVSI) for development in the relatively flat desert region west of Blythe, California. The Project is located just northwest of the Blythe Municipal Airport. Portions of the project site lie within the Airport Influence Area (AIA) as defined by the Riverside County Airport Land Use Commission (ALUC). The California Energy Commission and the RCALUC are concerned with the potential impact of thermal plumes from BSPP air cooled condensers (ACCs) on aircraft flight safety at the Blythe Airport. For the BSPP ACCs, the concern is that the thermal updrafts and turbulence associated with the fan-driven thermal plume coming off the ACC finned heat exchangers will interfere with aircraft stability at the Blythe Airport if an aircraft were to overfly a thermal plume. Four ACCs proposed for the BSPP, one for each of the four power blocks. None of the ACCs will be located within the Blythe Airport AIA but one will be close to the AIA boundary. To address CEC and RCALUC concerns, PVSI initiated a modeling study of the thermal plume from an ACC located in the desert environment. A companion study documents the results of a light aircraft flyover of a similar ACC at an operating power plant in a desert environment.

Air cooled condensers are used in energy generation systems to reject heat to the atmosphere, which acts as a large heat sink. Solar energy generating systems such as the BSPP are often located in desert environments where cooling water is in short supply. Because of the limited water supply for cooling needs, air cooled condenser (ACC) systems are used to recondense the steam for reuse in the steam cycle.

During operation, an ACC releases a large amount of thermal energy into the surface meteorological boundary layer above the ACC. Being warmer than the surrounding air, the release of thermal energy creates a thermal plume that can potentially cause turbulence above the ACC that could affect flight safety. However, any such thermal plume will be released into a desert environment that is subject to the natural occurrence of convective thermal plumes that result from the intense insolation that occurs in a desert location on a sunny day. Thus, an ACC has the potential to contribute additional turbulence to the already existing natural turbulence associated with convective thermals. It should be noted that solar power plants operate during the daytime where there is available sunlight. Consequently, the ACCs only have the potential to affect flight safety during daylight hours when they are operating.

While four ACCs are proposed for operation at the BSPP, three are well away from the AIA boundary, while the fourth is located near the AIA boundary. However, the traffic pattern at the Blythe Airport, as shown in Figure 1-1, does not pass over or near any of the proposed ACC locations. The RCALUC is proposing to establish a right hand pattern for Runway 26, and the approximate location of this revised pattern is indicated on Figure 1-1. Even when directed towards the BSPP, the new pattern does not take any aircraft close to any of the BSPP ACCs.

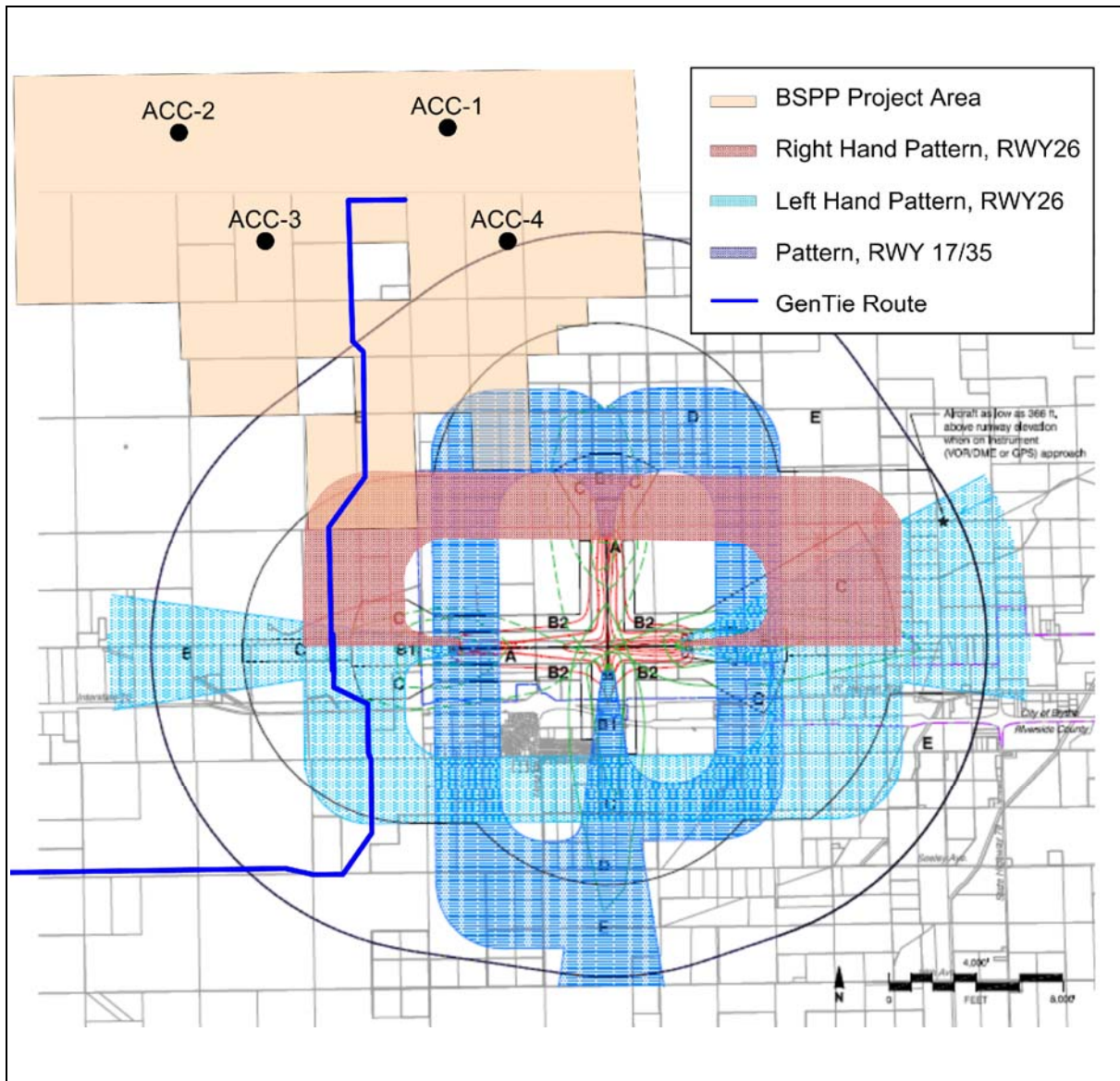


Figure 1-1. Current and Proposed Traffic Patterns at Blythe Airport Representing Approximately 80 Percent of Average Traffic.

1.1 Statement of the Problem

There are three deviations from stable flight that are of primary concern for this analysis:

1. aircraft pitch,
2. aircraft roll, and
3. aircraft vertical acceleration.

Pitch is measured by the angular rotation about the lateral (pitch) axis. The lateral axis passes through the aircraft from wingtip to wingtip. Roll is measured by the angular rotation about the longitudinal (roll) axis. The longitudinal axis passes through the aircraft from nose to tail. Vertical accelerations, and the resultant changes in altitude that result from the forces producing these accelerations can be simplistically referred to as turbulence.

The CEC and RCALUC have expressed concern that the thermal plume from the ACC could produce potentially significant changes in flight stability, as reflected in pitch and bank angles as well as contribute to additional turbulence that could adversely affect flight safety. The worst-case potential impacts are postulated to occur during summer midday when the BSPP is operating at maximum capacity under low ambient wind speed conditions. The CEC has established average vertical velocity as the metric to evaluate the impact of thermal plumes on flight safety and have established a significance threshold of 4.3 meter per second (m/s). The CEC has not established significance criteria relating to pitch, bank, or vertical acceleration.

1.2 Approach

This study involves an atmospheric modeling and data analysis effort to identify worst case meteorological conditions and to estimate the mean velocities and turbulence that will determine perturbations to expected flight characteristics. The main objective of this study is to develop and exercise a modeling effort to quantify the atmospheric impacts of the ACC designed and proposed by SPX Cooling Technologies, Inc. (Wyndrum, 2009). A first step is to gather information to develop a conceptual model and a modeling protocol to apply this conceptual model. Observations and the conceptual model are then used to develop inputs for a suitable computation fluid dynamics (CFD) modeling effort. The results of the modeling are used to determine potential impacts of the BSPP ACC on flight stability of aircraft operations near the Blythe Airport. This report documents this CFD modeling effort and its findings.

Prior observations of thermally and mechanically driven plumes have been examined to determine thermal plume characteristics in a convective unstable boundary layer such as will occur during full operation of the BSPP on a given day. Work by researchers such as Briggs (1975) have identified characteristic low horizontal wind speed, stagnant, and free convection conditions as likely culprits for producing plume maximum vertical velocities in the boundary layer from thermal plumes such as an ACC plume. To assess the occurrence of such conditions, midday radiosonde balloon released from Edwards AFB in the southern California Mojave desert were examined to determine the frequency and characteristics of low surface wind speed conditions (e.g. less than 1 m/s).

Such conditions are then modeled using the physical layout of the proposed BSPP ACCs. The modeling provides estimates of the vertical velocities and turbulence potentially affecting the flight characteristics. The modeling will explore unanticipated, but possible complicating meteorological factors that simply have not been captured by direct observation.

2.0 Development of a Conceptual Model

The proposed Blythe Solar Energy Project will be located in the southern California Colorado desert near Blythe, California. The desert location of the project will have a significant influence on the potential impact that thermal plumes from the ACC would have on flight safety at the nearby Blythe Airport. In particular, the clear sunny days during which the Project will operate at much of the year will produce a convective unstable boundary layer that is characterized by extensive thermal convection through a deep boundary layer. The purpose of this section is to bring together and present information from meteorology, thermodynamics and energy generation engineering studies to develop a consistent and rational model of the thermal plume from the ACC in a convective boundary layer. We begin with a review of some prior studies.

2.1 The Convectively Unstable Boundary Layer

The convectively unstable boundary layer has a negative bulk Richardson number and Monin-Obukhov length. Under such conditions the friction scaling velocity is no longer the characteristic velocity scale. Instead the convective scaling velocity, w^* is the more important typical velocity for convective motions.

Table 2-1 presents a summary of typical boundary layer meteorological parameters describing free atmospheric convection and their typical values under conditions expected at midday in Blythe, CA on a sunny summer day.

Table 2-1. Summary of Values.

Quantity	Typical value
Monin-Obukhov length	-5 m
Bulk Richardson number	-1.0
Convective scaling velocity	2.0 m/s
Horizontal wind direction standard deviation (Sigma theta)	30 degrees
Convective mixing height	3,000 m

The overall picture of air motions and dispersion indicates that convective elements move past a fixed point as a series of rolls and thermal plumes. Thermal updrafts interposed between convective thermal rolls are constrained to a smaller set of more intense updrafts, while compensating downdraft velocities are more modest and cover a larger area.

Observation studies of chimney plumes under such conditions indicate that even for elevated stacks the plumes from power plants with much greater momentum and buoyancy per unit area than an ACC plume perform 'looping' motions which bring plume material with high concentrations to the ground as 'blobs' of excessive pollutant concentrations. Remote sensing LIDAR data, air quality observations and meteorological observations from studies such as the EPRI PMV&D program in the 1980's confirm such behavior (Moore, Milich, and Liu, 1988). If such fossil fueled power plants plumes with their larger magnitude fluxes 'loop' then those of the ACC should be even further 'buried' in the

convective motions of the boundary layer thermals and will be advected by such motions. Given the small mass fluxes and low height with respect to the typical convective cell, it is equally likely that the ACC thermal plume is 'trapped' in the bottom portion of a convective cell and may move horizontally after immediate release as opposed to rising abruptly. An example of plume trajectory (shape) as it advects downwind in the convectively unstable boundary layer is given in Csanady (1973) who presents the descriptive figure shown as Figure 2-1.

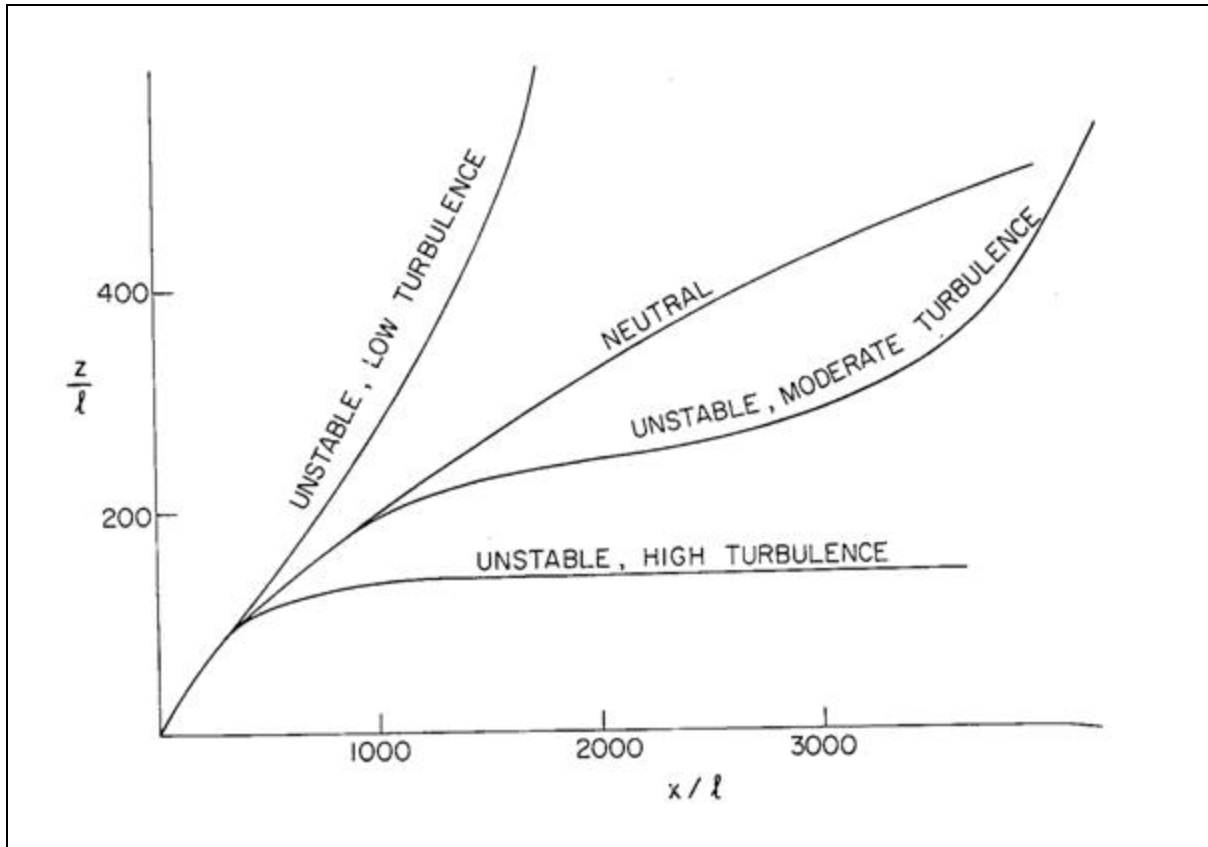


Figure 2-1. Qualitative illustration of normalized plume trajectories (plume shape) in the unstable boundary layer (courtesy of Csanady , 1973)

A previous CFD study was conducted on behalf of the California Energy Commission. This study is documented in Van Rooyen and Kroger (2008) and concentrated on the efficiency for heat dissipation of the system of fans in an ACC of very similar design to that proposed. A review of the study revealed that the atmosphere the fans were exhausting into was neutral and non convective. Even in their sensitivity cases 4 and 5, the analysis did not consider winds lower than 3 m/s and a non-neutral non-uniform wind profile. The findings were concentrated on the local efficiency of fans across the ACC array and issues such as how design features (e.g., walkways and skirts) affect the localized wind flow and hence heat dissipation. The rise of the ACC thermal plume away from the fan outlets and skirt under a buoyant atmospheric surface layer was not studied.

2.2 Plume Rise Analysis

The physical characteristics of the proposed ACC for the BSPP are given in Table 2.2. A schematic diagram of an ACC cell is given in Figure 2-2. The proposed BSPP ACC is composed of a 5x9 array of 45 individual fan cells.

Table 2-2. Physical characteristics of the ACC proposed for the BSPP

Physical Parameter	Units	Value
Condensing Duty	MMBtu/hr	1,379
Steam Turbine Exhaust Flow	lb/hr	1,510,515
Steam Turbine Exhaust Enthalpy	Btu/lb	1,003.1
Steam Turbine Exhaust Pressure	in HgA	3.691
Inlet Air Dry Bulb Temperature	°F	96.7 (@17% RH)
Site Elevation	Ft	471
Number of Modules		45
Unit Length	m	114
Unit Width	m	74
Unit Height	m	36.6

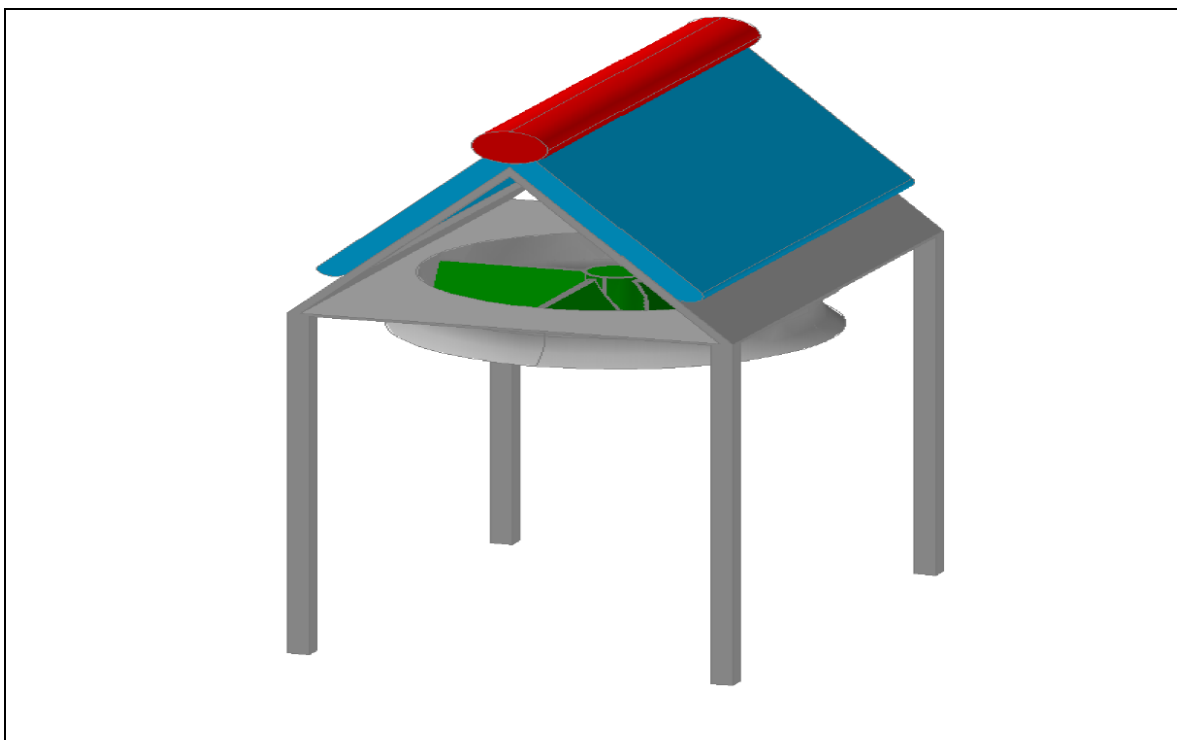


Figure 2-2. Schematic diagram of a typical ACC cell showing axial fan (green), fan shroud (gray), supporting structure (dark gray), steam header (red), and heat transfer tubes (blue)

The ACC thermal plume has a very modest temperature excess of 10 deg K, a modest average initial exit velocity of 4.5 m/s, and an overall effective fan area of 6,685 m². The computed buoyancy flux, F , of the ACC under full load is of the order 2887 m⁴/s³. In his authoritative mini-monograph (Chapter 8) discussion of Plume Rise Briggs (1975) discusses light wind conditions under convectively unstable conditions. Under such conditions, plume rise will follow a general relationship in which the rise of the plume is proportional to the downwind distance to the 2/3 power, typically called the “2/3 power law”. Briggs indicates that there is no lower limit on the horizontal wind speed, U , in the 2/3 law relation for plume rise. The vertical movement of plume mass rises at the rate of increase of the plume centerline rise with time. Thus a simple screening tool of the vertical plume rise speed, w , is the formula.

$$\langle w \rangle = (1.6)(0.66)(F/Ut)^{1/3}$$

If one assumes that it takes 60 seconds for the exhaust air to reach 300 m with an average wind speed of 2 m/s, then the vertical velocity of the plume centerline by the time it reaches 300 m is 3 m/s, a value significantly below the 4.3 m/s threshold of interest defined by the California Energy Commission as a significance threshold for potential impact on aircraft flight stability.

Because the horizontal wind speed, U , appears in the denominator in the equation for vertical velocity, w , the presumption is that worst-case vertical motion and plume rise will occur under calm wind conditions. However, Briggs (1975) argues like Tennekes (1971) did that (page 94) there is some lower limit to the horizontal wind speed in the convectively unstable boundary layer:

“There is a limiting factor though, and that is that the atmosphere never holds still in the presence of convection. There is some minimum effective U that is due to convective motion, so it is proportional to w_* .”

For this analysis, we have selected a low, but not zero horizontal wind speed to simulate the convective boundary layer. This horizontal is characterized by a wind speed at 100 meters of 2 m/s, with near calm conditions at the surface. It should be noted, however, that the proposed BSPP ACC is 120 ft (36m) high, the plume released from it will be unlikely to experience true calm winds.

2.2.1 Model Selection

Field monitoring data on plume rise from an ACC operating in a desert environment are not available. A modeling analysis of the ACC plume rise is therefore necessary to quantify the potential impact on aircraft flight stability of the thermal plume produced by an ACC. Such modeling can provide estimates of the vertical velocities and turbulence affecting the flight characteristics. The modeling can also explore unanticipated, but possible complicating meteorological factors that simply have not been captured by direct observation. The use of models also allows an examination of the no-build case to see what maximum perturbations to the flight environment might be.

Wind tunnel experiments are most accurate under near neutral turbulence conditions. Under extreme diabatic conditions such as low wind speed under free convection, fluid flow wind tunnel modeling approaches become less accurate and realistic. A numerical approach represented by computation fluid dynamic (CFD) models is a reasonable alternative. Reynolds Averaged Navier-Stokes (RANS) numerical models have recently proven themselves, when applied properly, to be realistic models of turbulent flow (Meroney, 2004).

In recent years there has been a proliferation of RANS CFD models described in the scientific literature but only a few commercial models offer an operational capability that make it possible for technical staff other than the model developers to successfully apply the codes to real world problems. AECOM currently utilizes the commercially supported FLOW-3D and FLUENT CFD models, both which have internal consistency checking and adequate documentation to allow both accuracy and flexibility for a wide variety of fluid applications. The FLUENT CFD was used by Van Rooyen and Kroger (2008) in their study for the CEC. One reason for the selection of FLUENT CFD by Van Rooyen and Kroger was the ability to generate a complex surface grid mesh to explicitly represent the complexity of the fan structure in great detail. While this may be of advantage for structural design studies, it is expected to carry a resource penalty when studying the global atmosphere in more detail.

For this study, the FLOW-3D model was selected for the present analysis owing to its ability to rapidly generate an appropriate modeling mesh, and numerical efficiency to rapidly exercise a number of numerical tests. These are needed to ascertain the accuracy and sensitivity to various model control and input options such as boundary and initial conditions, fluid thermodynamics, and forcing options. FLOW-3D also has both a user friendly interface as well as sophisticated visualization system to view model predicted parameters as profiles, slices, surface, trajectories, vectors, etc. When configured in a similar manner, the two CFD models have been shown to give qualitatively similar results).

3.0 Description of the Modeling Environment

This section summarizes the overall environment of the proposed BSPP. The Project location and environment have been selected for maximum solar power production in a location where electrical grid infrastructure is available. The environment is a dry desert environment where latent heat perturbations to modeled airflows can safely be ignored. During the midday when the ACC is expected to be running at full capacity, the atmosphere in the first few 10's of meters is quite unstable. This is evidenced by the frequent occurrence of thermals and dust devils during summer afternoons near Blythe.

3.1 Geographical Data

The location of the proposed facility is just to the north northwest of the Blythe Airport (BLY) centered at 710312 m easting and 3727562 m northing in UTM zone 11 using WGS-84 (NAD83). An annotated satellite image of the region of interest is shown in Figure 3-1. The northern end of Blythe Airport Runway 35 is visible in the bottom. The pushpin shows the proposed location of the ACC of concern to this study. The distance from this unit to the northern most tip of Runway 35 is approximately 4,380 m.

The United States Geological Survey (USGS) seamless digital terrain data base was accessed to obtain 10 m resolution Digital Elevation Model (DEM) data which is displayed in Figure 3-2 as contours. The Environmental Protection Agency (EPA) National Landuse Cover Data (NLCD) 25 m high resolution land use data was accessed and the land cover is displayed in Figure 3-2 as well. From Figure 3-2 several important points can be noted. The first is that for upwards to several kilometers around the proposed site the terrain is rather flat and slopes gently upwards to the northeast. The second is that the land use in the area is primarily desert shrub land with some bare rock and sand. The satellite imagery of Figure 3-1 suggests that the shrub coverage is very sparse so that the roughness is small and the desert most closely resembles a sandy desert with little vegetation.

The motivation of the modeling effort is to determine the impact of the proposed facility on the flight characteristics of general aviation activity at Blythe airport. Figure 3-3 shows the footprint of the various airport compatibility (exclusion) zones near to the location of the ACC. The closest project ACC to these compatibility zones is shown in Figure 3-1 by the pushpin.



Figure 3-1. A satellite image of the proposed ACC site. The northern tip of the Blythe Municipal Airport is shown at the very bottom adjacent to old irrigation circles

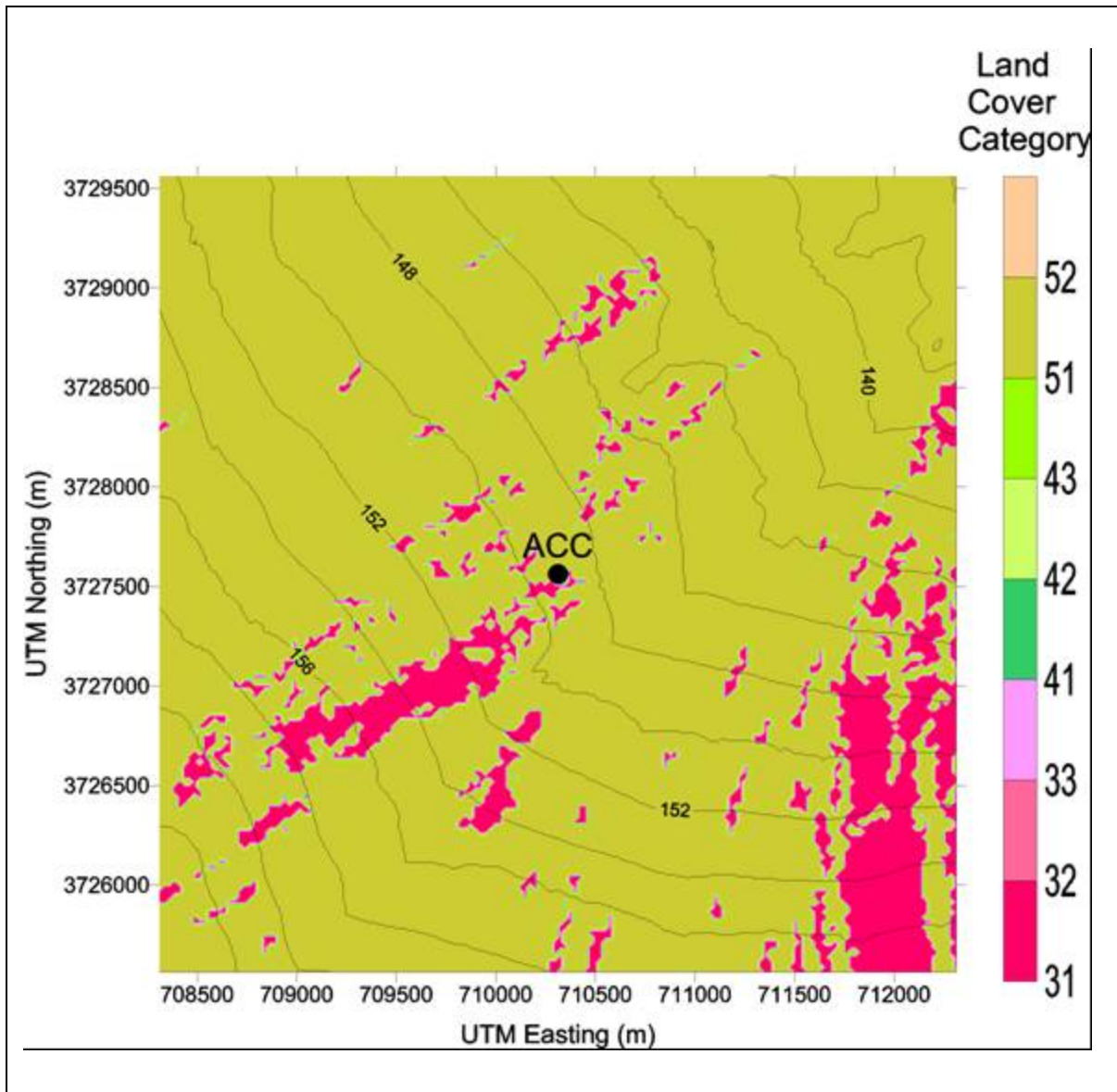


Figure 3-2. A plot of the terrain and land cover category within 2 km of the proposed ACC

The terrain contours are in m. The land use categories are desert shubland (51) and desert bare rock sand and clay (31). The proposed location of the air cooled condenser in the closest power block to the airport is labeled ACC.

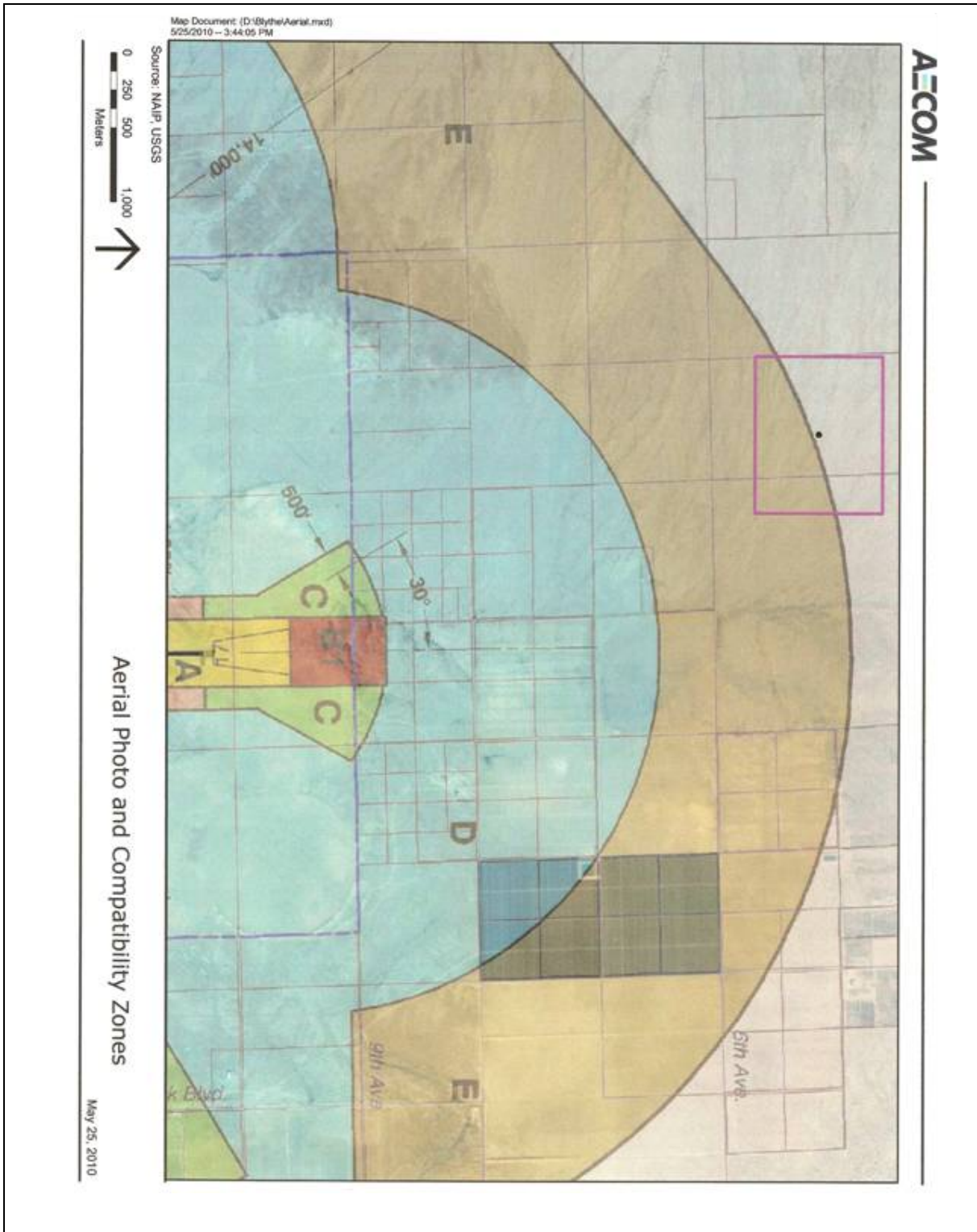


Figure 3-3. An image plot overlaid by the FAA exclusion zones and the location of the proposed ACC

3.2 Meteorological Characteristics

As noted in the previous section, the region of concern is primarily sandy desert. The main source of local meteorological data is the National Weather Service (NWS) Automated Surface Observing System (ASOS) airport data at Blythe Airport (BLH) and upper air twice daily rawinsonde data (00Z and 12Z) at desert sites in the southwest like Edwards AFB, CA, and Tucson, AZ. In this section we analyze the available data for midday summer periods when winds are low and there is likely to be a deep convective boundary layer.

The thermal turbulence and updrafts are most likely to be largest under midday conditions when the ACC is in full operation. While calm conditions are more likely to occur under morning and evening transition conditions, we will consider both to occur simultaneously for the sake of maximizing the perturbation of the ACC thermal plume on the ambient atmosphere. In this section we present the wind profiles that are used as part of the CFD modeling.

3.2.1 Surface Data Analysis

The Blythe Airport (BLH) ASOS data was processed into surface and profile files for AERMOD. These files contain hourly averaged data. Figure 3-4 shows the wind rose for Blythe during the middle of the day. The Figure shows that the most frequent winds are out of the southeast quadrant. These most frequent wind directions would direct a thermal plume away from the exclusion zone. Given the proposed location shown in Figure 3-3, the thermal plume would fall outside of the exclusion zone.

Calms are found to occur about 11% of the time during the day in the Blythe ASOS data. However, the reporting threshold for ASOS wind speed is 3 knots and thus the 11% value represents the occurrence of winds of less than 3 knot, not just calm winds. In addition, experience in conducting prior meteorological analysis of calm and missing wind occurrence indicates that the frequency of calm winds is significantly reduced when the 5 and 2 minute ASOS wind data is used in the analysis. A reduction in the frequency of very low or calm winds is can typically be reduced by up to a factor of four by review of the shorter period observation data. However, as stated above, ASOS reported calm winds actually refer to winds of less than 3 knots.

3.2.2 Upper Air Analysis

Wind tower data is not present in the Blythe study area. So instead we have selected radiosonde observations from Edwards AFB (WMO 73281). Data were taken from the National Oceanic and Atmospheric Administration (NOAA) Integrated Global Radiosonde Archive (IGRA) archive for only those soundings that occurred during the midday during June through August for the period 1990-2010. In addition we reduced our sample size further by looking for only those soundings whose release wind speed is less than 1.0 m/s in the first level (approximately less than 10 m above the ground). The greatest uncertainty in wind speed occurs due to tracking uncertainty right at release. Furthermore, the wind observation is an instantaneous one and not an hourly average, which most likely is larger since persistent winds less than 1 m/s are relatively rare in open terrain.

Only a handful of rawinsondes had release speeds of 1 m/s or less. These profiles are displayed in Figure 3-5. In this Figure two groups of profiles can be noted: soundings that clearly occurred earlier in the day with lower inversion heights and cooler surface temperatures, and those that occurred in the heat of the day with no clear sign of a capping inversion in the first 1,000 m. A composite sounding used for the present study is denoted as 'MEAN'.

The wind speed profiles are shown in Figure 3-6. A zero wind speed suggests that the balloon ascended nearly straight up, whereas the 0.5 m/s balloons showed evidence of horizontal drift, even if

it was rather small. The composite profile used in the present study is denoted as 'MEAN'. It assumes a wind speed at 100 m of 2 m/s based on an assumed constant bulk Richardson number of the order -1 and a Monin-Obukhov length of -5 m (See Table 2-1). Under stagnant conditions with no pressure gradient driven mean wind the power law in the surface layer goes as the square root of the height. Above the surface layer the height power law reverts to the more usual smaller convective values. An exponent of 0.25 seemed to make sense when plotted against the radiosonde profiles in Figure 3-6.

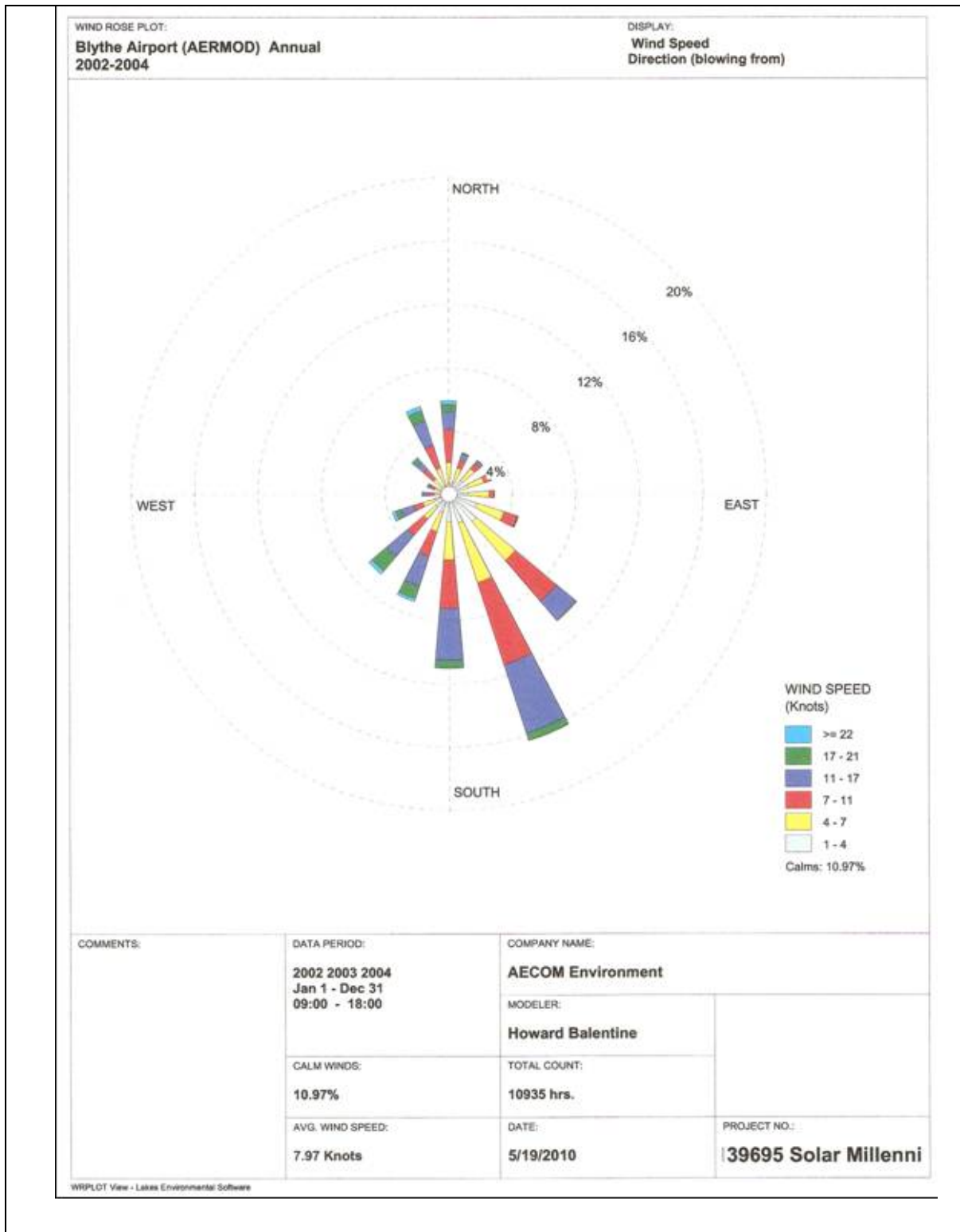


Figure 3-4. Wind rose of the ASOS (10 m hourly) winds at the Blythe Municipal Airport (BLH) during the hours 0900-1800 LST

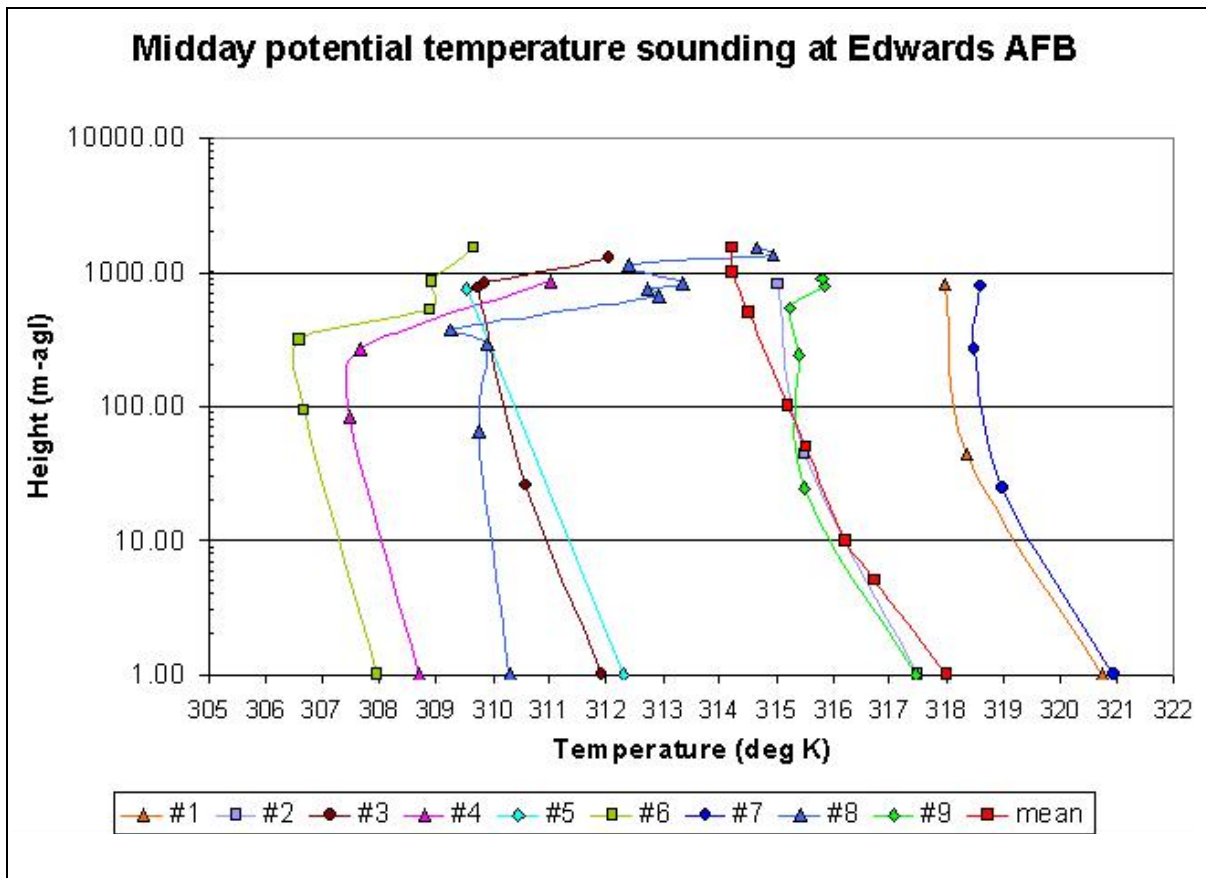


Figure 3-5. Vertical profiles of potential temperature observed from mid-day rawinsondes released at Edwards AFB during June-August with wind speeds less than 1.0 m/s in the first reporting level (1990-2010)

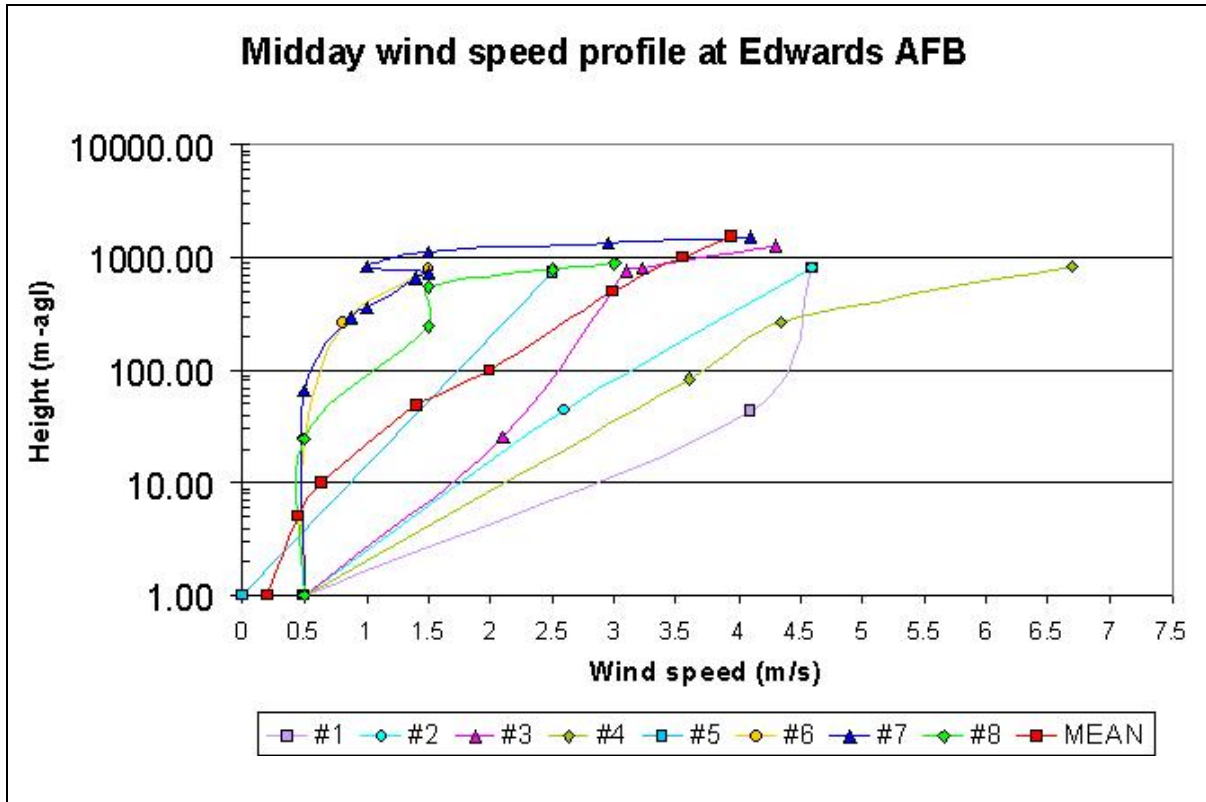


Figure 3-6. Vertical profiles of wind speed observed from midday rawinsondes released at Edwards AFB during June-August with wind speeds less than 1.0 m/s in the first reporting level (1990-2010)

3.3 Surface Calm Conditions

An important question is how hot does the surface (skin) temperature of the desert actually get? Observations suggest that for dry sandy soils of the Arizona Sonoran desert, the temperature in the surface exceeds 60° C (333° K). The vertical temperature gradients in air above the soil in the first meter are quite steep, as shown in Figure 3-7. A simple heat budget model based on the approach of Gaffin et al. (2007) and Oke (1987) suggest that for the soils in the area a surface skin temperature of 337 deg is typical.

The atmosphere is said to be calm when the mean wind (e.g. an hourly average) is less than some minimum value say either 0.5 m/s or the instrument stall speed. Calm winds are associated with extremes of atmospheric stability such as extremely stable or unstable conditions in the surface layer or with transient conditions associated with the movement of a convergent or divergent weather system such as a front. A near zero wind speed suggests a transient decoupling of a layer of the atmosphere from the rest of the atmosphere such as in the case of gravity driven slope flows where the wind profile indicates a change in direction by 180 degrees abruptly at some point. Regardless of the meteorological condition, calms occur for a limited time and over a limited vertical extent of the atmosphere.

In the convective boundary layer, the mean field wind supplies energy for mechanically driven turbulence while insolation provides energy for thermal convection. The relationship between mechanically driven turbulence and thermal turbulence can be described by the Bulk Richardson Number, the ratio of thermally produced turbulence to turbulence generated by vertical shear. If the

surface layer were truly calm throughout its full extent, the definition of such a layer would fail, similarity and convective boundary layer theory would fail and the mixing length hypothesis would fail as well. In this case, by definition the Richardson number could not be estimated. If however one assumed that under measured calm conditions at a height of 10 m that the Richardson number was constant in a strongly convective mixed layer then one could estimate an effective vertical wind shear. Turning the bulk Richardson number definition around and assuming a zero wind speed at the surface the variation of horizontal wind U with height would be proportional to the square root of the height z ,

$$U(z) = Kz^{1/2}$$

where the constant K is given by

$$K = [(g/\theta)(\Delta\theta/Ri)]^{1/2}$$

where θ is the potential temperature, g is the gravitational constant, and Ri is the Richardson number. The change in potential temperature is measured across z . If we assume that similarity still holds and the Monin-Obukhov length L is negative and small (e.g. -5 m) at the height where the calm is observed (e.g. 10 m) then according to the Businger relation.

$$Ri = [0.47\zeta (1 - 15\zeta)^{1/4}]/[1 - 9\zeta]^{1/2}$$

where $\zeta = z(\text{calm})/L$. For a 10m height we have $\zeta = -2$ and Ri is approximately -0.8 . For an ambient potential temperature of 310° K, and a measured superadiabatic lapse rate of -1° K per 100 m we estimate a wind speed of the order 2 m/s at the top of the first 100 m of a steady and bulk homogeneous atmosphere even if calm winds are observed in the first 10 m.

Above the stagnant surface layer the convective planetary boundary layer has coupling to the moving air aloft. The convective regime has a power law wind speed profile closer to 0.1 reflecting a relative constancy with height. For the region between 100 m and 1,000 m an exponent of 0.25 was used after looking at several rawinsonde profiles.

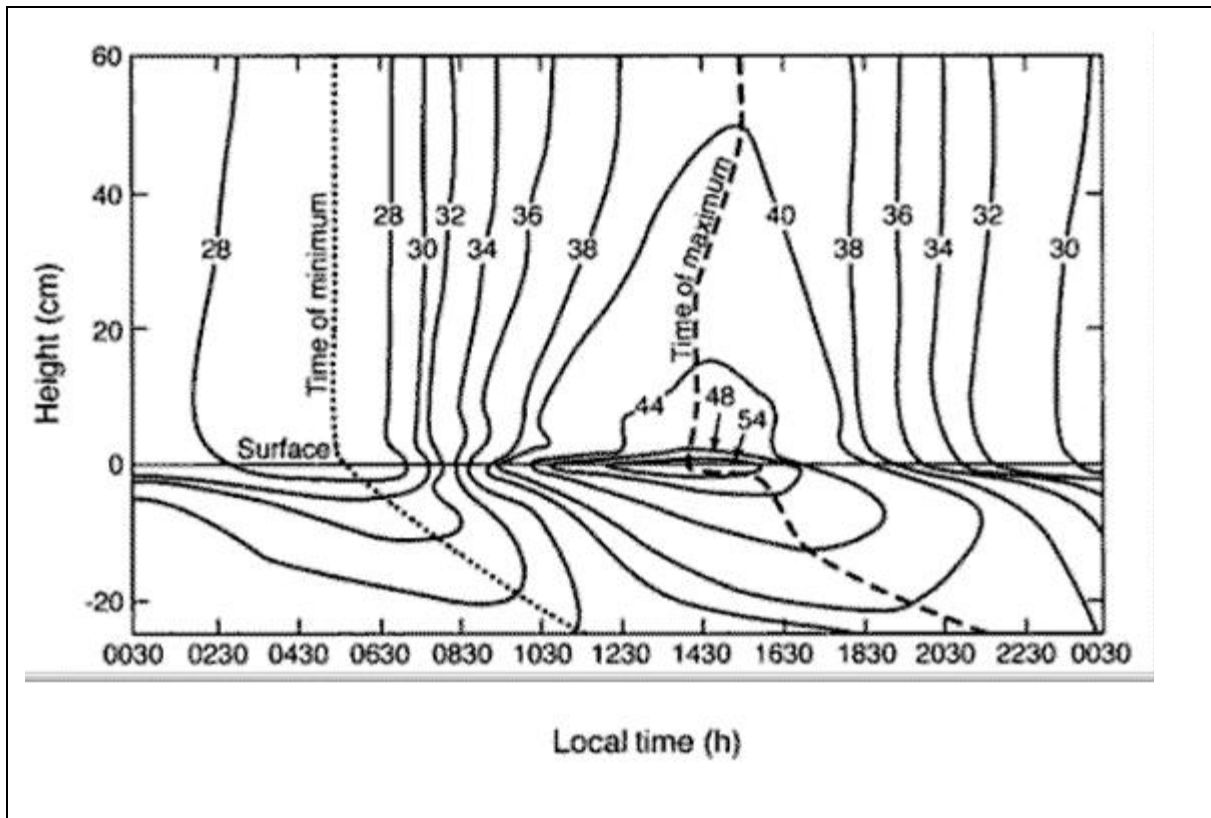


Figure 3-7. The temperature ($^{\circ}\text{C}$) just above and below the surface of sparsely vegetated sandy plains in the Sonoran Desert, averaged for July and August 1956. The dashed and dotted lines define the time of the temperature maximum and minimum at each height or depth. Note the non-uniform isotherm interval. (Adapted from Dodd and McPhelimy, 1959.)

4.0 CFD Model Input Preparation

The atmosphere in the FLOW-3D CFD model was operated as a Boussinesq (incompressible) fluid. Pressure is allowed to vary at the model top, but is fixed at the bottom. Temperature and pressure were supplied along the inflow boundary assuming hydrostatic equilibrium. Temperature was supplied as potential temperature to provide the proper vertical density gradient and to provide for a proper energy equation. A negative temperature gradient at the bottom of the modeling grid provides an energy source for the convective turbulence. In addition a vertical profile of the TKE boundary and initial conditions was applied. A series of simulations were conducted with and without the vertical profile of horizontal wind speed on the inflow and at the top of the mode. The bottom boundary is a no slip one. The temperature at the bottom boundary (1 m) was set to a constant value (318 deg K) over the domain except at the top of the ACC.

In this section the following subjects are addressed;

- Physical layout of the ACC, collector array, and modeling domain
- Boundary and initial conditions
- Model grids

In addition to these topics we describe some of the metrics used to estimate perturbations of flight characteristics such as pitch, banking, and roughness..

4.1 Physical Layout of the ACC and Modeling Domain

There are three different modeling sub-regions in the proposed CFD exercises. The outer coarse domain describes convectively unstable desert thermal internal boundary layer (TIBL) at equilibrium. The land use is unimproved, sandy desert. The middle region represented the solar mirror array surrounding the ACC. The innermost region was represented by a high resolution mesh consisting of a footprint describing the ACC fans and A-frame slotted/finned heat diffusers. The solar array region covers an area of approximately 1050 m in the east-west direction and 850 m in the north-south direction. The physical layout is presented in Figure 4-1. Some simplifications were made to expedite the modeling. For example a square collector array area is assumed for purposes of symmetry in modeling the collector array. The rectangle is replaced by a square 950 m on a side.

Figure 4-1 shows the N-S lines of collector arrays. The arrays are separated by the width of an access road to (1) allow transport into the array for maintenance and (2) to avoid having one set of collectors 'shading' another at low sun angles. The collectors have an aperture of 6.7 (22 ft) and pointed vertically their lip stands at 7.62 m (25 ft) above the ground (Figure 4-2). There are 14 rows of collectors oriented S to N to the west of the ACC and 19 rows to the east of the ACC.

The height of the A frame cooling panels extends from an edge 23.1 m above the ground to 36.5 m at the peak of the A frame steam feeder tube. The footprint of the ACC array extends 77 m by 113 m. The drawings of the proposed fans were converted into CAD drawings which are then used to render the ACC in the refined mesh. These CAD drawings are presented in Figure 4-3.

4.2 Development and Application of Boundary and Initial conditions

The bottom boundary temperature was developed for each of the sub regions. As mentioned in Section 3, these can be estimated from a simple heat balance model. The surface roughness is a another physical parameter that had to be estimated for each sub region.

4.2.1 Surface Material Characteristics

In order to establish the surface model inputs for the CFD modeling, a number of physical parameters were needed. The surface (skin) temperature was estimated for each of the materials assuming no thermal storage. For ground surfaces the daily heat penetration by conduction is approximately 15 percent of the net radiation.

Table 4-1. A summary of the physical surface characteristics used in the present modeling study.

Material	Roughness (m)	Albedo	Bowen Ratio	IR Emissivity	Heat Conductivity (w/m-K)	Max Surf Temp (K)
Dry desert sand	0.05	0.30	8	0.85	0.25	345
Gravel	0.02	0.25	3	0.93	1.00	341
Concrete	0.001	0.40	10	0.89	0.29	338
Asphalt	0.01	0.10	10	0.95	0.75	348
Aluminum mirror	0.00001	0.94	25	0.10	250	348
Aluminum condenser	0.00001	0.55	25	0.10	250	360
Collector canopy EW	0.64	0.34	10	0.66	81.0	NA
Collector Canopy NS	0.25	0.34	10	0.66	81.0	NA

The estimation of the roughness of the collector array was done by first assuming a canopy depth, H_c , determined by the obstacle heights and that $z_o = 0.05H_c$. The collector canopy height was set at 7.6 m leading to an initial estimate of 0.38 m (38 cm) for a shallow canopy. However the ratio of canopy height to drag length scale $H_c/L_c = \sim 1$ when the sectional drag is $C_d = 5$ so that the canopy can be considered to be deep like a forest. Using the Kung relation $\log(z_o) = -1.24 + 1.19\log(H_c)$ we find the roughness is of the order 0.64 m. Along the rows (S to N) there is no gap and the canopy is shallower with the smaller roughness..

The surface coverage of the collector array is assumed to be a mix of gravel (roadway) and aluminized collector surface. The fractions of coverage are 68 percent gravel and 32 percent aluminized surface at no tilt. From the EW side the fraction of the side canopy is 33 percent open (under the supports) and 67 percent closed (by the collector surface). From the NS the fraction open is 79 percent and closed is 21 percent. The collector canopy entries are estimated as the weighted sum of gravel and aluminum mirror.

The ground temperatures range from 337 – 345° K. or 64 – 75° C. This is a temperature sometimes observed in an extreme desert environment. Dull metal like the condenser plates could become dangerously hot to the touch when the ACC is not working.

4.2.2 Input Boundary and Initial Conditions

At the model top the vertical velocity could be nonzero allowing material to enter and exit the region. This was initially set to zero. At the bottom both the initial and boundary condition set the vertical velocity to zero. At the top and bottom of the modeling domain both temperature and pressure are held fixed. The inflow boundary conditions for pressure are estimated from the temperature profile and the hydrostatic relation. Potential temperature was estimated from temperature and the Exner function. The density profile was estimated from the equation of state. The turbulent kinetic energy (TKE) was estimated using an assumption of a power law vertical profile to adjust values of σ_θ and σ_ϕ for height. At the reference height (10m) a value of 30 degrees was used for σ_θ and 10 degrees for σ_ϕ .

The vertical profile of TKE was given by

$$\sigma_u = (\sigma_\theta/u)(10m/z)^{0.06}$$

$$\sigma_w = (\sigma_\phi/u)(z/10m)^{0.02}$$

The power law exponents were taken from Pendergast (1984). The TKE was specified as

$$\text{TKE} = \sigma_u^2 + 0.5\sigma_w^2$$

The potential temperature, density, windspeed and TKE vertical profiles used for modeling are presented in Attachment 1.

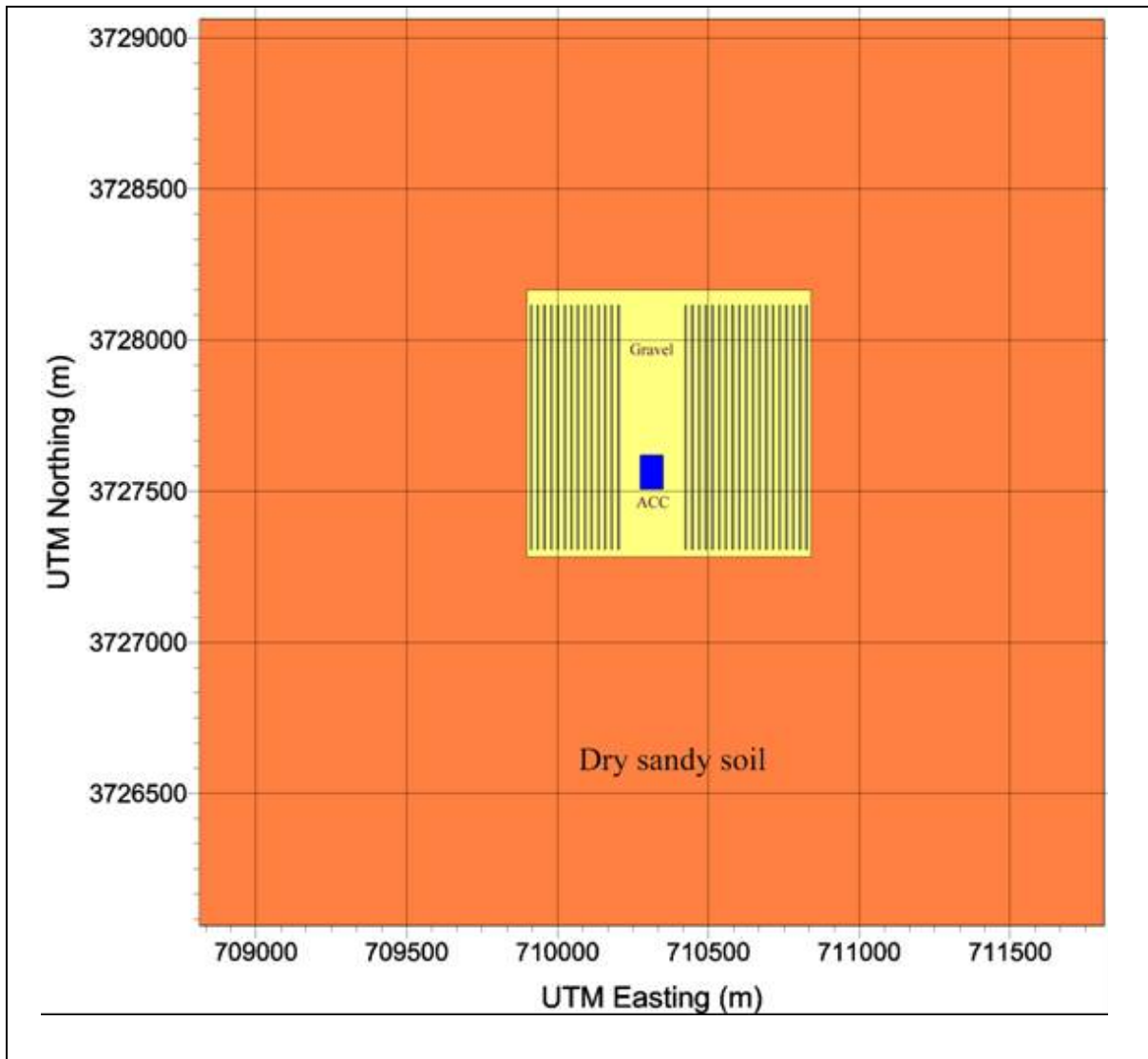


Figure 4-1. A plot of the three sub regions, desert, solar collector array, and ACC.



Figure 4-2. A picture showing a parabolic mirror solar array at the Kramer Junction SEGS plant

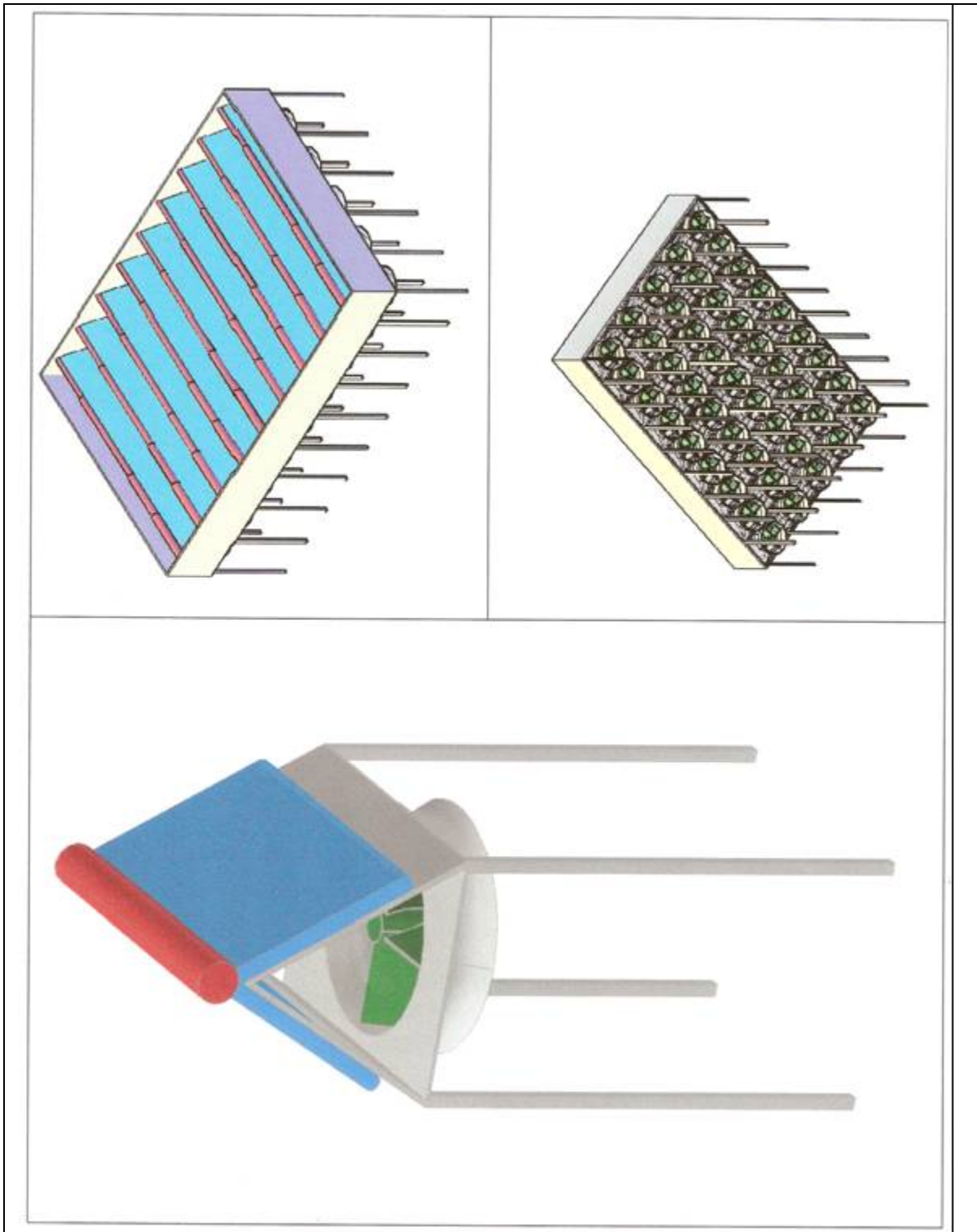


Figure 4-3. Graphical CAD renderings of the ACC fan arrays, A frame tent array with wind screen, and single fan view of the A frame condenser assembly.

4.3 Determination of the Modeling Grid

The modeling grid went through several iterations. The final simulation contained 150 layers with each being 10 m thick. The horizontal grid for a coarse outer grid extends from 1500 m upwind and downwind of the ACC. This modeling domain has a grid cell size of 150 m. This region equilibrates the inflow boundary conditions. An inner computational domain uses a variable size mesh with cells ranging from 10 m to 150 m. The ACC surface is introduced as a series of intermediate (finer) cells at the center of the modeling domain. An X-Z plot of the outer portion of the finer computational mesh is shown in Figure 4-3. The inner portion which is even more refined is shown in Figure 4-4.

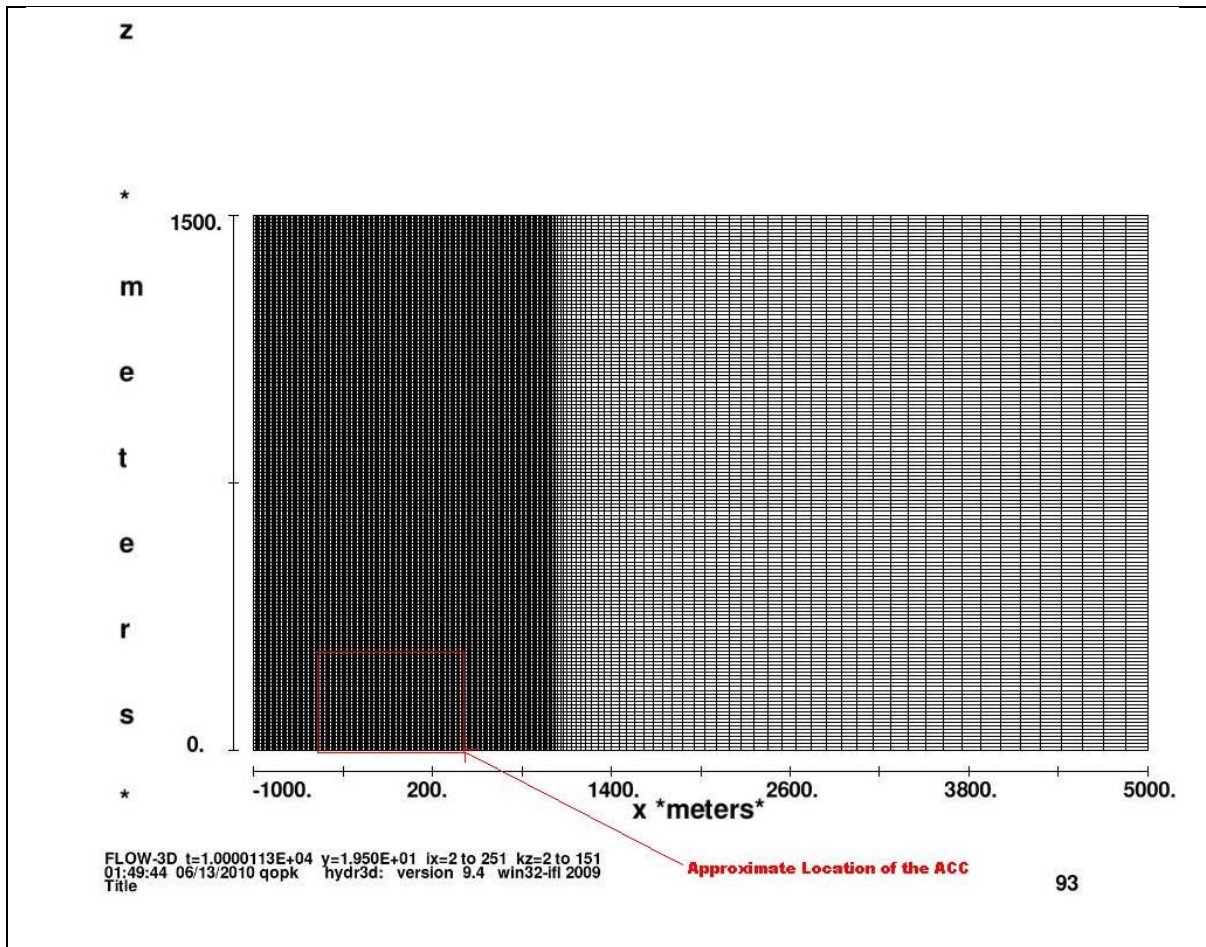


Figure 4-3. X-Z side view of the modeling domain mesh used in the present study.

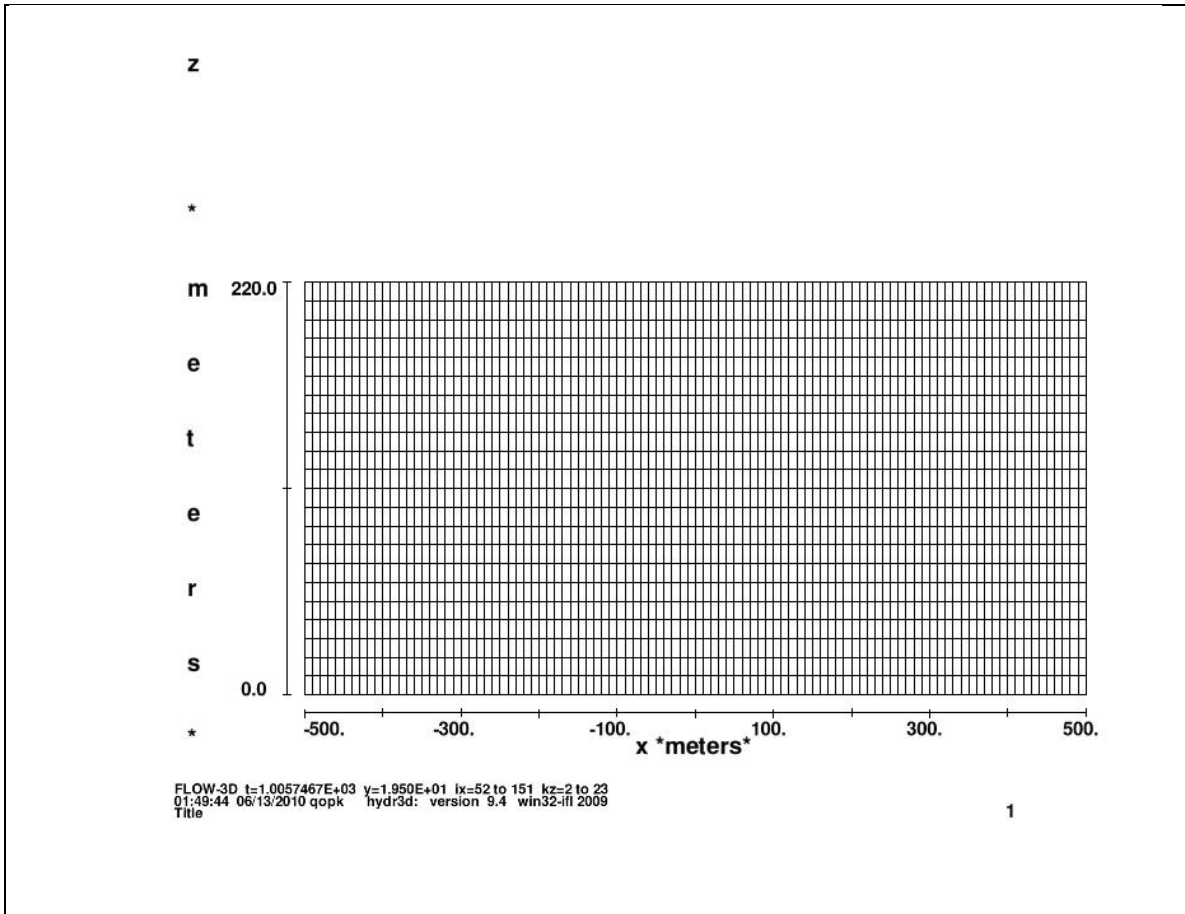


Figure 4-4. Magnified X-Z side view of the modeling domain mesh used in the present study centered on the ACC.

5.0 WIND 3-D Application and Analysis

The FLOW-3D CFD was exercised in a phased manner based on the degree of simplification and realism. In phase 1 the model was exercised for calm conditions with a single fan and a simplified smooth surface. This was followed by a series of simulations using several increasingly sophisticated grid meshes designed to resolve the modeling scenario with increasing realism. In a final set of simulations, the ACC was modeled with a high resolution solid body representation of the CFD fan housings and skirt with the full fan configuration.

5.1 Description of Simulations

During the study of the ACC's impact, a number of simulations were made, each with an increasing level of realism. The ACC and collector arrays were modeled using symmetry and a simple roughness. Variations in terrain and land cover were ignored and the physical layout of the ACC flow characteristics was simplified.

Table 5-1. A summary of CFD simulations

	Simulation Description		
Phase 1	Environment	Source	Layout
Case 1	Zero horizontal wind, +3 deg surface, constant aloft	+ 10 deg C, no mass flux	One fan no screen, no collectors zone
Case 2	Zero horizontal wind, +3 deg surface, constant aloft	+ 10 deg C, mass flux	One fan no screen, no collector zone
Phase 2	Environment	Source	Layout
Case 1	Wind, TKE profile, +3 deg surface, +2 degree 1000-1500m	+10 deg C, mass flux	Fans and collector zone, no screen
Case 2	Wind, TKE profile, +3 deg surface, constant aloft	+10 deg C, mass flux	Fans and collector zone, no screen
Phase 3	Environment	Source	Layout
Case 1	Wind, TKE profile, +3 deg surface, constant aloft	+10 deg C, mass flux	All ACC and power block structures, collector array for one power block.
Notes: Wind – horizontal wind speed of 2 m/s at 100 m TKE – vertical profile of boundary layer total kinetic energy +3 deg surface – surface temperature is 3 deg C above air temperature immediately above Constant aloft – TKE profile is constant			

5.2 Visualization of Simulation Results

The results of the model simulations were analyzed via several forms of visualization. The most useful is a slice in the X-Z plane passing through the center of the ACC and parallel to the wind inflow. This allows a straight forwards examination of the ACC thermal plume maximum perturbations to the airflow and how they decrease with height. Vertical profiles of layer maximum and minims of key parameters were plotted to provide an indication of the magnitudes of quantities that would affect flight characteristics.

5.2.1 Idealized Simulations

The preliminary idealized simulations consisted of simple no-wind (calm) simulations with the observed temperature/density profile. They were performed to evaluate the model setup and energy balances of the Phase 3 final simulations and represented steady-state simulations at equilibrium. However, due to the difficulty in creating such a simulation in the limited time available for this study, the calm simulations were not judged to be credible and are not presented.

5.2.2 Final Simulation (Phase 3)

The Case 1 Phase 3 simulation results produced a looping convective field. The boundary layer for this simulation is represented by a super adiabatic lapse rate near the surface that gradually transforms into a unstable layer in the middle part of the modeling domain, and eventually transforms into a neutral layer at the top of the modeling domain. The focus of the analysis is on the vertical wind velocities in the first 500 m that can be expect to be generated under such convectively unstable conditions. A visualization of the wind field in a sub-domain around the ACC is shown in Figure 5-3. This figure represents a 'snapshot' of the vertical velocity field at 2,000 seconds into the simulation through an X-Z (west-east) cross section passing through the middle of the ACC. The ACC does not produce positive vertical wind above 250 m of greater than 2 m/s. There are no winds exceeding 4.3 m/s (colored red in Figure 5-3) anywhere in the domain except within a few 10's of meters immediately above the ACC. One should note that as the plume moves down stream there are several convective loops that produce local maximums in the vertical velocity at heights above 250 m, however none of these exceed 2 m/s.

Figure 5-4. shows the vertical profile of layer maximum and minimum vertical wind speed. The up and down motions are associated with the rising and descending portions of the thermal boundary layer produced by the convective cells in that boundary layer. The simulation shows that the upward vertical wind speed decreases linearly with height to less than 2 m/s at and above 150 m) above the ground (approximately 490 ft, well below the pattern altitude at the Blythe Airport of 800 ft). The maximum vertical velocity occurs at the ridge top of the A frame. Below the top of the ACC there is some evidence of a rotor in the lee of the ACC with nearly equal upwards and downwards branches. Above 150 m there is some oscillation of the maximum upwards vertical velocity possibly corresponding to an upwards assist by the ACC, but the contribution is of the order of fractions of a meter per second.

Figure 5-5 displays the horizontal wind speeds. On the inflow side the wind profile ranges from fractions of a meter per second near the surface to over 3 m/s aloft. The impact of the ACC thermal plume and the ACC and collector array is to create a surface stagnant region near the surface and to create a slightly rising outflow jet aloft. This jet aloft is associated with a residual plume density deficit as shown in Figure 5-6 and indicates that the plume retains residual buoyancy while passing through the wake turbulence region downwind of the ACC structure. Even under small inflow wind speeds the plume shows limited rise and a tendency to push the thermal plume from the ACC downwind. Once

the thermal plume departs the wake region of the ACC structure, the density deficit contributes to rise of the ACC plume.

5.2.3 Impact on Flight Characteristics

The total g-force experienced by a plane depends on the plane's mass, speed, and the horizontal gradients in the vertical velocity field the aircraft is flying through. There is a 'static' g-force felt by the plane due to a vertical acceleration of the air it is flying in, even if it were not moving forwards. There is also a dynamic g force experienced by the plane as it flies through air moving upwards and downwards. This g-force depends on the horizontal gradient of the vertical velocity as well as the speed of the aircraft. The response time, or frequency, represented by the spatial and temporal resolution of the boundary layer scaling is 10 seconds, representing the time for a cycle of deflection and restoration to complete. Consequently, the temporal resolution available from the modeling results is half of the response time, or 5 seconds. Thus, for the current simulation, the temporal resolution is 5 seconds for a pitch motion or a bank change produced by an imbalance of the thermal plume acting on an airframe. The effects on an airframe represent the imbalance of forces, with part of the airframe within the thermal plume and the other part outside. For example, a change in bank angle would be introduced where one wing was within the ACC plume and the other is outside, resulting in an imbalance in lift, with a resulting bank of the aircraft. This situation would be most pronounced adjacent to the ACC where the thermal plume would be relatively compact.

Estimated airframe departures in pitch, bank angle, and vertical motion, representative of a 5-second period, are presented in Figures 5-5 to 5-7. The 5-second resolution is a limitation of the temporal and spatial resolution in the modeling simulation. Because of the relatively coarse temporal resolution of 5 seconds, somewhat higher frequency fluctuations of shorter duration can be expected. However, revised modeling at a greater temporal and spatial resolution would be required in order to resolve these higher frequency events. Based on the current simulations that demonstrate small magnitude departures of the flight stability metrics, and results from the companion aircraft flyover of an operating ACC that likewise observed only minor impacts of an ACC thermal plume on flight stability, revised modeling simulations with a finer temporal and spatial resolution are not expected to produce significantly different results than those presented below.

Figure 5-5 shows the profile of change in pitch as a function of height above the ground for an aircraft with an air speed of 35 m/s (approximately 80 mph). This airspeed is representative of an aircraft configured to land with landing gear down and flaps extended. The result is that at an airspeed of 80 mph, the maximum departure from level flight would be of the order of 2-4 degrees, averaged over 5 seconds.

The vertical upward and downward g-forces associated with the ACC plume alone over a 5-second period were estimated and the layer maximum and minimum g-forces are plotted in Figure 5-6. The maximum g-forces are less than a tenth of a g. The simulation shows that the g-force profiles are symmetric, as would be expected only if updrafts equal downdrafts in scale and intensity. It should be noted that this condition is usually not the case in free convection in the planetary boundary layer and down drafts are often weaker and cover a greater area.

The modeled change in bank angle while flying over the ACC is illustrated in Figure 5-7. The resulting change in bank angle over a 5-second period is less than one degree and is not likely to be noticed by a pilot flying in the convectively unstable boundary layer simulated.

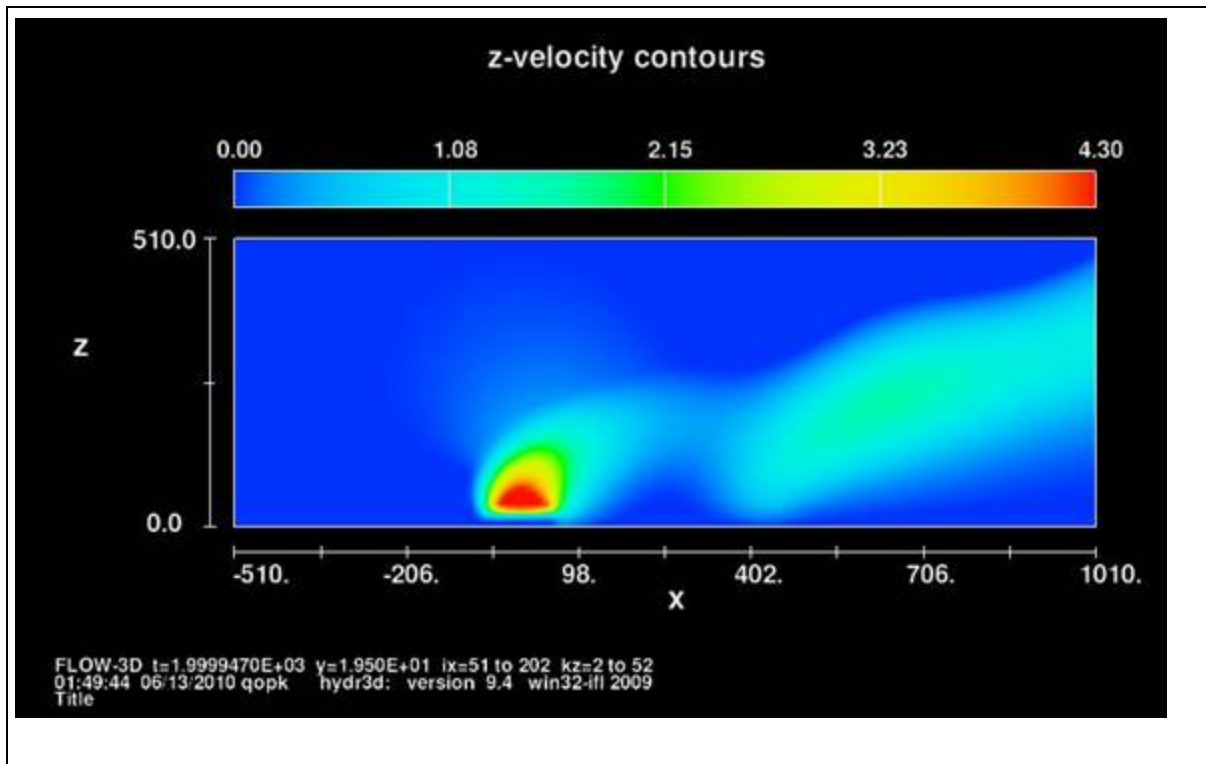


Figure 5-1. A snapshot of the X-Z cross section of upwards directed (positive) vertical wind speed at 2000 seconds into the simulation in a convectively unstable boundary layer resulting in a looping plume. The ACC is in the range (-39,39)

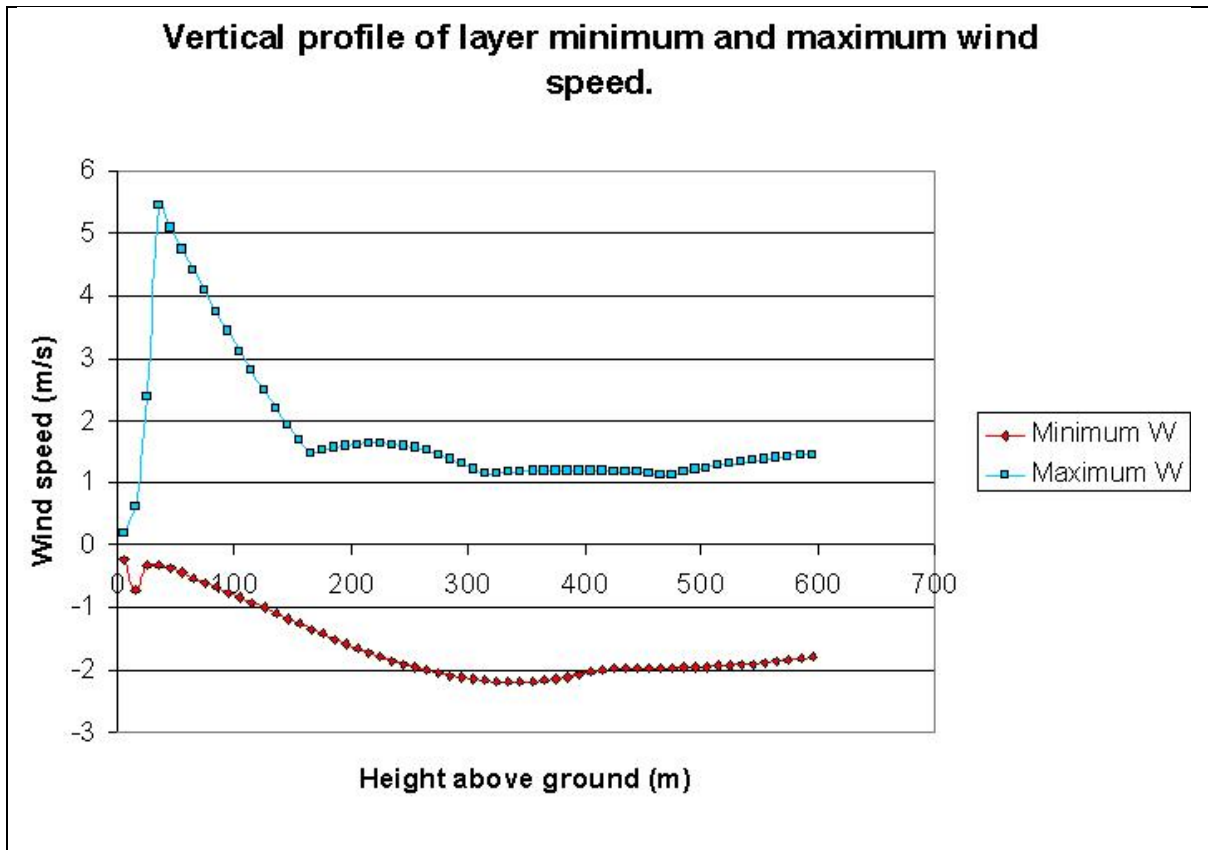


Figure 5-2. A vertical profile of minimum and maximum vertical wind speed found in each model layer (10 m layers)

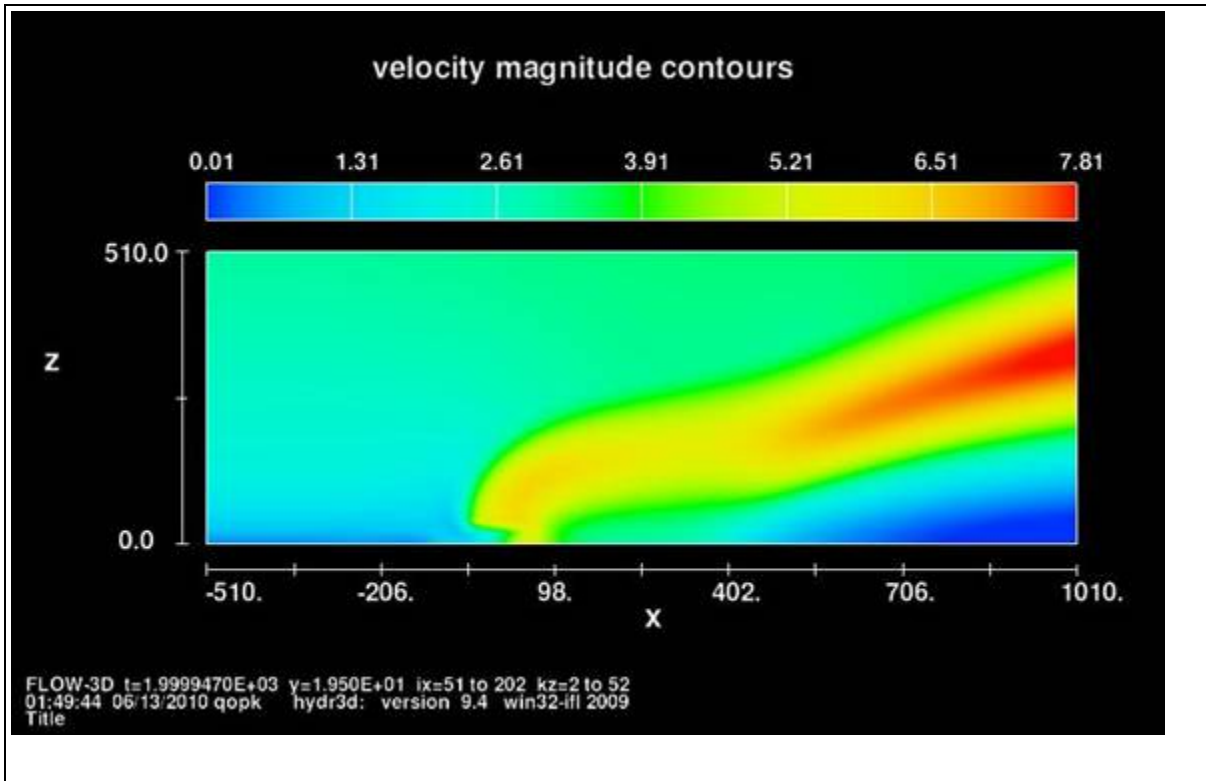


Figure 5-3. An X-Z cross section snapshot showing the horizontal wind speed (m/s) in the immediate vicinity of the ACC at 2,000 seconds into the simulation. The ACC is in the range (-39,39)

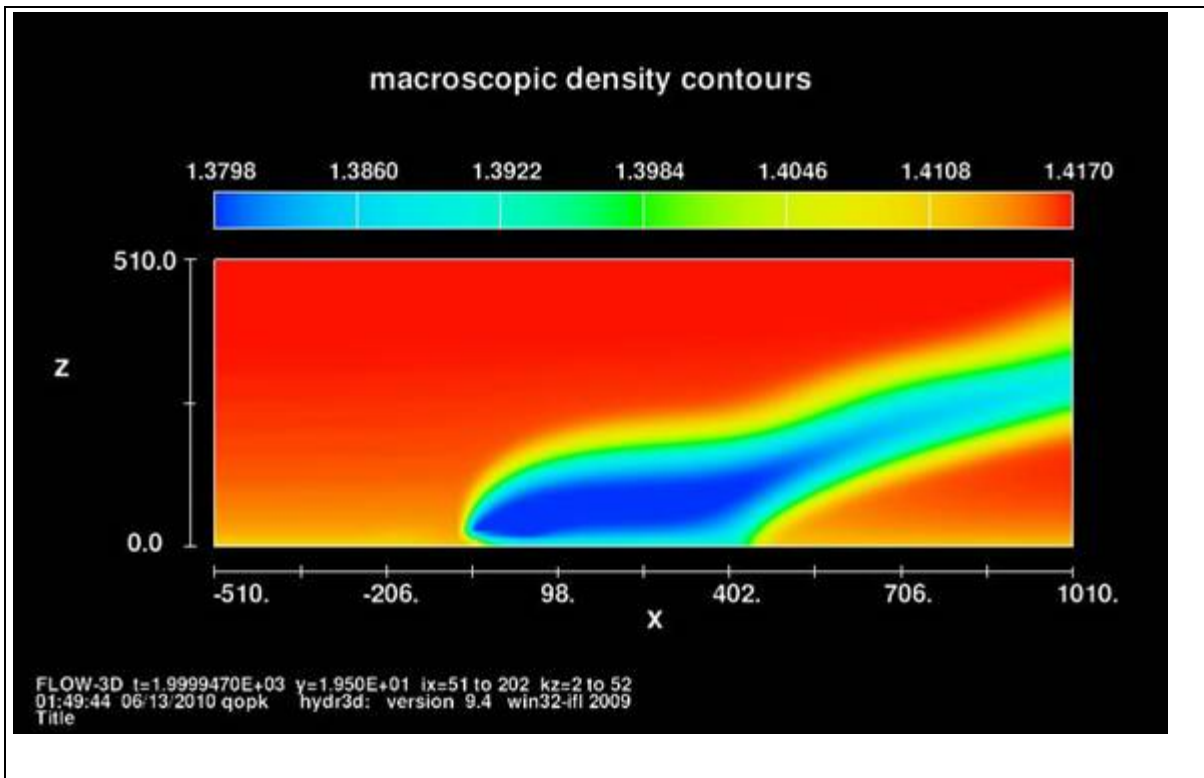


Figure 5-4. An X-Z cross section snapshot showing the air density profile (kg/m³) in the immediate vicinity of the ACC at 2,000 seconds into the simulation. The ACC is in the range (-39,39)

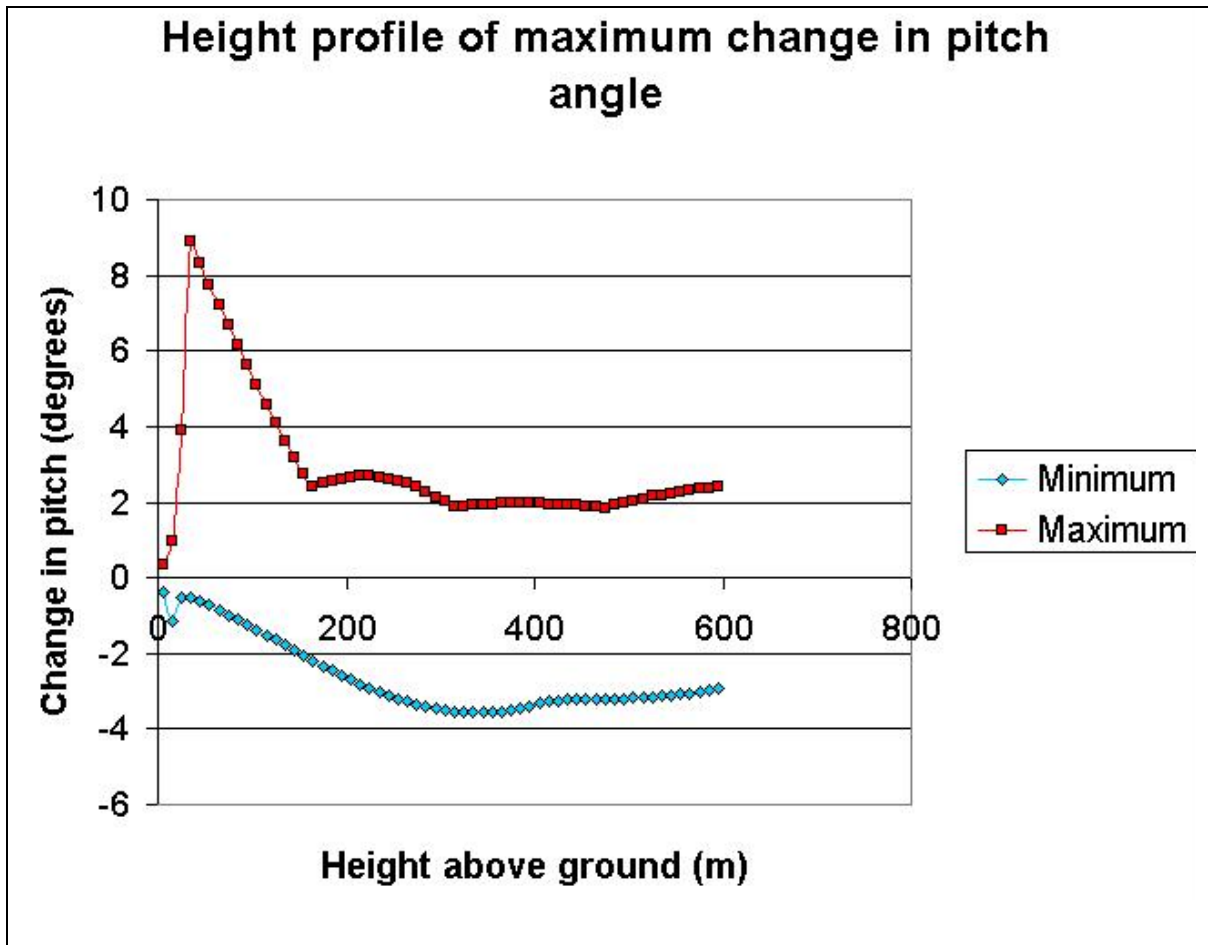


Figure 5-5. The profile of maximum change in aircraft pitch angle as a function of height above the ground experienced by an aircraft at 80 mph (35 m/s) due to the ACC thermal plume alone over a 5 second period and absent the influence of the boundary layer convective

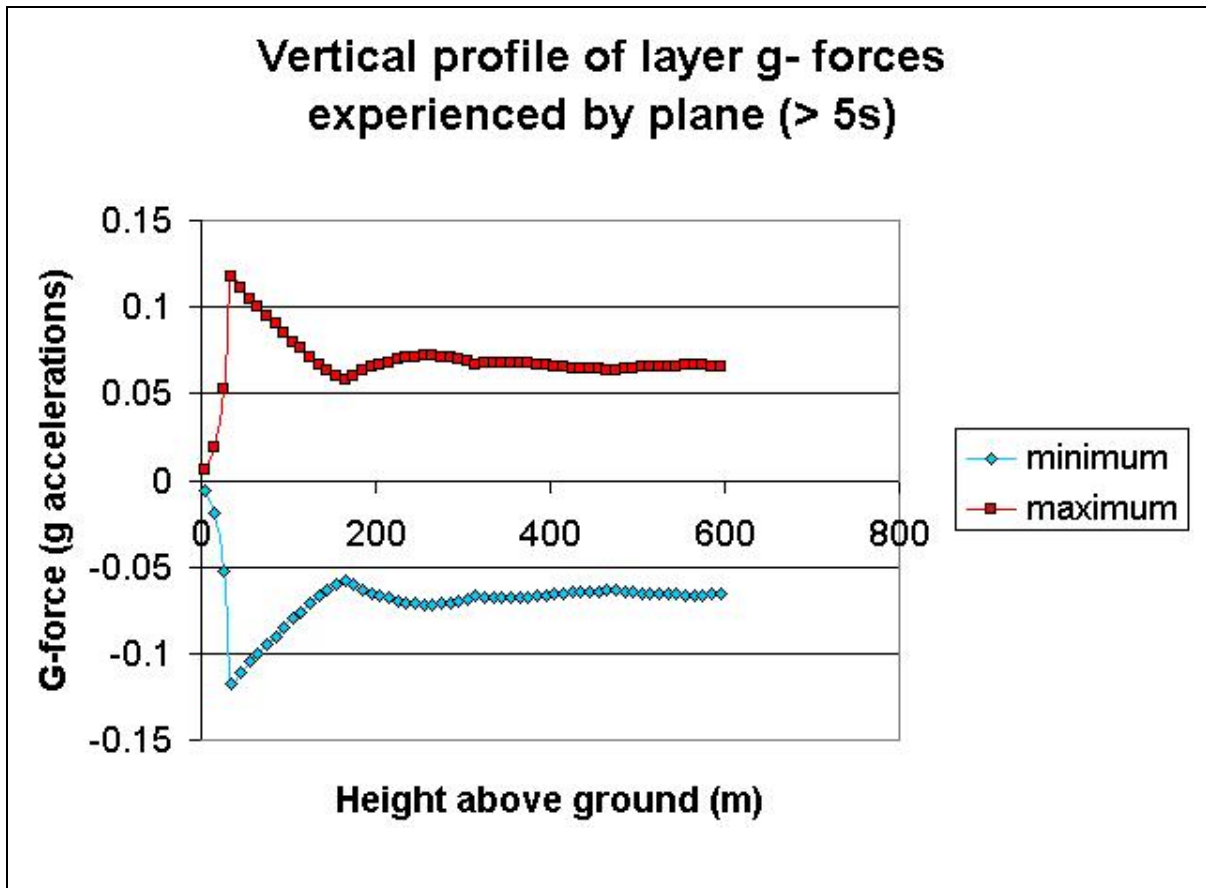


Figure 5-6. The vertical profiles of g-force accelerations as a function of height above the ground experienced by an aircraft at 80 mph (35 m/s) due to the ACC thermal plume alone over a 5 second period and absent the influence of the boundary layer convective

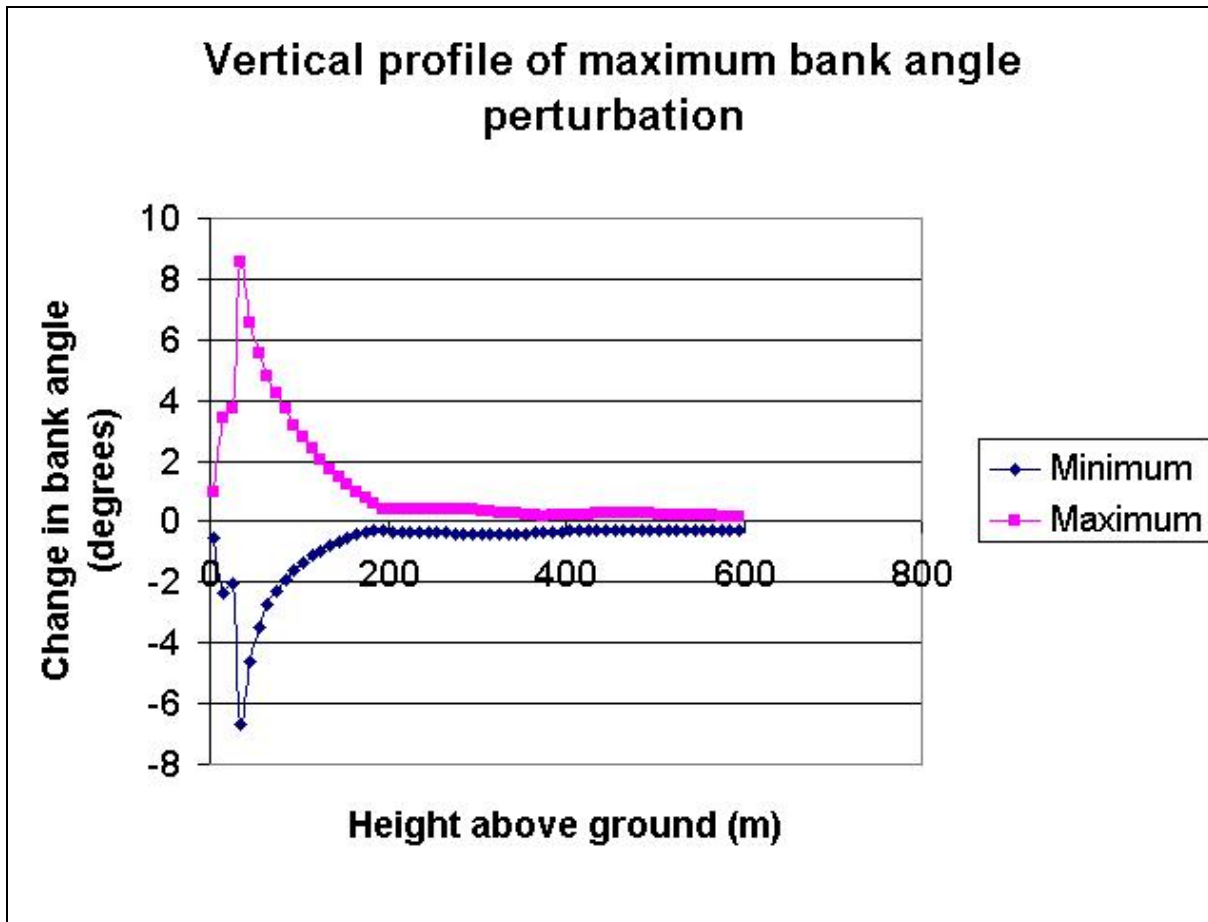


Figure 5-7. The vertical profiles of the maximum change in bank angle as a function of height above the ground experienced by an aircraft at 80 mph (35 m/s) due to the ACC thermal plume alone over a 5 second period and absent the influence of the boundary layer convective

6.0 References

Pasquill, F and F.B. Smith, 1983. Atmospheric Diffusion – 3rd Edition, Ellis Horwood Limited, John Wiley and Sons, New York, NY

Briggs, G.A., 1975. Plume Rise Predictions (Chapter 8 in lecture on Air Pollution and Environmental Impact Analyses, Workshop Proceedings, American Meteorological Society, Boston, MA pp 59-111.

Randerson, D. , 1984. Atmospheric Boundary Layer (section 5) from Atmospheric Science and Power Production (D. Randerson editor), Technical Information Center, United States Department of Energy, DOE/TIC 27601.

Van Rooyen, J.A., and D.G. Kroger, 2008. Performance Trends of an Air Cooled Steam Condenser Under Windy Conditions, California Energy Commission, CEC-500-2007-124, Sacramento, CA.

Csanady, G.T., 1973. Turbulent Diffusion in the Environment, D. Reidel Publishing Company, Boston, MA

Tennekes, H., 1973. Similarity Laws and Scale Relations in Planetary Boundary Layers (section 5) Workshop on Micrometeorology, American Meteorological Society, Boston, MA pp 177-218.

Businger, J., 1973. Turbulent Transfer in the Atmospheric Surface Layer (section 2), Workshop on Micrometeorology, American Meteorological Society, Boston, MA pp 67-100

Moore, G.E., J.B. Milich, and M.K. Liu, 1988. Plume Behaviors Observed Using Lidar and SF6 Tracer at a Flat and Hilly Site, Atmospheric Environment, Vol 22(8), pp.1673-1688.

Liu, M.K. and G.E. Moore, 1984. Diagnostic Validation of Plume Models at a Plains Site, Electric Research Power Institute. (EPRI) EA-3077., Palo Alto, CA.

Wyndrum, R., 2009. (client confidential communication). Technical Memorandum on Budgetary Proposal for Air Cooled Condenser for Solar Millennium 240 MW Solar Power Plant Blythe, CA.

Belcher, S.E., N. Jerram, and J.C.R. Hunt, 2003. Adjustment of a Turbulent Boundary Layer to a Canopy of Roughness Elements, Journal of Fluid Mechanics, Vol 488, pp 369-398.

Attachments

Attachment 1. Inflow Boundary Layer Parameter Profiles

Below are given the boundary layer meteorological parameters at the inflow boundary used in the final simulation.

Ht Height above Ground (m)
 Pres Pressure (mb)
 Rho Air Density (kg/m³)
 Temp Air Temperature (°K)
 TKE Total Kinetic Energy (m²/s²)

Ht (m)	Pres (mb)	Rho (kg/m³)	Temp (degK)	Ws (m/s)	TKE (m²/s²)
1	997.017	1.092463	317.9902	0.2	1.50E-02
3	996.8021	1.095254	317.1118	0.34641	3.98E-02
5	996.5869	1.096466	316.6928	0.447214	6.25E-02
7	996.3716	1.097208	316.4102	0.52915	8.43E-02
9	996.1563	1.09772	316.1942	0.6	0.105406
11	995.9408	1.097981	316.0508	0.663325	0.125976
13	995.7253	1.098063	315.9586	0.72111	0.146138
15	995.5098	1.09811	315.8769	0.774597	0.16596
17	995.2943	1.098129	315.8029	0.824621	0.185493
19	995.0789	1.098128	315.735	0.87178	0.204777
20.875	994.8768	1.098111	315.6758	0.913783	0.222654
22.5	994.7018	1.098086	315.6273	0.948683	0.238006
24	994.5402	1.098056	315.5846	0.979796	0.25207
25.375	994.392	1.098024	315.5469	1.007472	0.264879
26.5	994.2708	1.097994	315.5171	1.029563	0.275302
27.5	994.1631	1.097965	315.4912	1.048809	0.284527
28.5	994.0554	1.097934	315.4659	1.067708	0.293715
29.5	993.9476	1.097901	315.4411	1.086278	0.302869
30.5	993.8399	1.097867	315.4168	1.104536	0.311989
31.5	993.7322	1.097831	315.393	1.122497	0.321076
32.5	993.6246	1.097793	315.3696	1.140175	0.330133
33.5	993.5169	1.097754	315.3466	1.157584	0.339159
34.5	993.4092	1.097714	315.3241	1.174734	0.348156
35.5	993.3015	1.097672	315.3019	1.191638	0.357125
36.5	993.1938	1.097629	315.28	1.208305	0.366067
37.5	993.0861	1.097585	315.2585	1.224745	0.374982
38.625	992.965	1.097534	315.2346	1.24298	0.384981
40	992.817	1.097471	315.2059	1.264911	0.39716

41.5	992.6555	1.097399	315.1753	1.28841	0.410394
43.125	992.4806	1.097319	315.1426	1.313393	0.424673
45	992.2787	1.097224	315.1058	1.341641	0.441077
47	992.0635	1.09712	315.0673	1.371131	0.458494
49	991.8483	1.097014	315.0296	1.4	0.475832
51	991.633	1.096904	314.9926	1.428286	0.493093
53	991.4178	1.096793	314.9563	1.456022	0.510282
55	991.2026	1.096679	314.9206	1.48324	0.527401
57	990.9874	1.096563	314.8855	1.509967	0.544454
59	990.7723	1.096445	314.851	1.536229	0.561443
61	990.5571	1.096326	314.8169	1.56205	0.57837
63	990.342	1.096205	314.7833	1.587451	0.595237
65	990.127	1.096082	314.7501	1.612452	0.612048
67	989.9119	1.095958	314.7173	1.637071	0.628803
69	989.6969	1.095833	314.6849	1.661325	0.645504
71	989.4819	1.095706	314.653	1.68523	0.662155
73	989.2669	1.095579	314.6213	1.708801	0.678755
75	989.052	1.09545	314.5899	1.732051	0.695306
77	988.837	1.09532	314.5589	1.754993	0.711811
79	988.6221	1.095189	314.5282	1.777639	0.72827
81	988.4073	1.095057	314.4977	1.8	0.744684
83	988.1924	1.094924	314.4675	1.822087	0.761056
85	987.9777	1.09479	314.4376	1.843909	0.777385
87	987.7628	1.094655	314.4079	1.865476	0.793674
89	987.548	1.09452	314.3784	1.886796	0.809922
91	987.3333	1.094384	314.3492	1.907878	0.826132
93	987.1186	1.094247	314.3201	1.92873	0.842304
95	986.9039	1.094109	314.2913	1.949359	0.85844
97	986.6892	1.093971	314.2626	1.969772	0.874539
99	986.4745	1.093832	314.2342	1.989975	0.890603
101.125	986.2465	1.093683	314.2042	2.005601	0.90257
103.625	985.9783	1.093507	314.1693	2.017884	0.911251
107	985.6163	1.093268	314.1226	2.034117	0.922771
111.75	985.1069	1.09293	314.0576	2.056326	0.93862
118	984.4368	1.09248	313.9731	2.084493	0.958865
125.75	983.6063	1.091916	313.8701	2.117908	0.983091
135	982.6156	1.091237	313.7493	2.155825	1.010855

145	981.5453	1.090495	313.6209	2.194684	1.039608
155	980.4756	1.089745	313.4945	2.231582	1.06719
165	979.4067	1.08899	313.3699	2.266736	1.093719
175	978.3386	1.08823	313.2468	2.300327	1.119295
185	977.2712	1.087465	313.1252	2.332507	1.144007
195	976.2047	1.086696	313.0048	2.363408	1.167926
205	975.1388	1.085923	312.8855	2.393142	1.191118
215	974.0737	1.085147	312.7672	2.421808	1.213639
225	973.0093	1.084368	312.6499	2.44949	1.235537
235	971.9457	1.083587	312.5334	2.476264	1.256858
245	970.8829	1.082803	312.4176	2.502197	1.27764
255	969.8209	1.082017	312.3026	2.527348	1.297918
265	968.7596	1.081229	312.1882	2.55177	1.317722
275	967.6992	1.080439	312.0745	2.57551	1.337083
285	966.6394	1.079647	311.9612	2.598611	1.356025
295	965.5805	1.078854	311.8486	2.621112	1.374571
305	964.5223	1.07806	311.7364	2.643047	1.392744
315	963.465	1.077264	311.6247	2.66445	1.410562
325	962.4084	1.076467	311.5134	2.68535	1.428043
335	961.3526	1.075669	311.4025	2.705772	1.445204
345	960.2975	1.07487	311.2919	2.725742	1.46206
355	959.2433	1.07407	311.1818	2.745283	1.478626
365	958.1898	1.07327	311.072	2.764415	1.494913
375	957.1372	1.072468	310.9625	2.783158	1.510935
385	956.0853	1.071666	310.8532	2.801529	1.526702
395	955.0342	1.070863	310.7443	2.819546	1.542225
405	953.9839	1.070059	310.6357	2.837225	1.557515
415	952.9344	1.069255	310.5273	2.854579	1.572579
425	951.8857	1.06845	310.4192	2.871622	1.587427
435	950.8378	1.067645	310.3113	2.888366	1.602067
445	949.7906	1.06684	310.2036	2.904825	1.616507
455	948.7442	1.066033	310.0962	2.921009	1.630753
465	947.6987	1.065227	309.9889	2.936928	1.644813
475	946.6539	1.06442	309.8818	2.952592	1.658692
485	945.6099	1.063613	309.775	2.96801	1.672397
495	944.5668	1.062806	309.6683	2.983193	1.685935
507.5	943.2639	1.061797	309.5352	3.00185	1.702627

522.5	941.7019	1.060585	309.3758	3.02379	1.722336
540	939.8818	1.05917	309.1902	3.048796	1.744906
562.5	937.5451	1.05735	308.9524	3.08007	1.77329
592.5	934.4353	1.054922	308.6363	3.120341	1.810097
630	930.5576	1.051886	308.2426	3.168583	1.854568
675	925.9186	1.048242	307.7723	3.22371	1.905889
725	920.7825	1.044193	307.2519	3.281818	1.960565
775	915.6664	1.040146	306.7335	3.336994	2.013028
825	910.5701	1.036102	306.2169	3.389561	2.063503
875	905.4937	1.032061	305.7018	3.439791	2.112181
925	900.4371	1.028025	305.1882	3.487911	2.159223
975	895.4003	1.023994	304.6758	3.534119	2.204769
1025	890.3835	1.019933	304.175	3.578582	2.248939
1075	885.3867	1.015846	303.685	3.621447	2.291841
1125	880.41	1.011768	303.195	3.662842	2.333567
1175	875.4532	1.0077	302.705	3.702878	2.3742
1225	870.5164	1.003643	302.215	3.741658	2.413813
1275	865.5995	0.999594	301.725	3.779267	2.452474
1325	860.7024	0.995556	301.235	3.815786	2.490239
1375	855.8251	0.991527	300.745	3.851285	2.527164
1425	850.9676	0.987509	300.255	3.885829	2.563297
1475	846.1298	0.9835	299.765	3.919476	2.598682

**STATE OF CALIFORNIA
ENERGY RESOURCES CONSERVATION AND DEVELOPMENT COMMISSION**

In the Matter of:
APPLICATION FOR CERTIFICATION
for the *BLYTHE SOLAR POWER PROJECT*

Docket No. 09-AFC-6
PROOF OF SERVICE
(Revised 1/26/2010)

APPLICANT

Alice Harron
Senior Director of Project
Development
1625 Shattuck Avenue, Suite 270
Berkeley, CA 94709-1161
harron@solar Millennium.com

Elizabeth Ingram
Developer, Solar Millennium LLC
1625 Shattuck Avenue, Suite 270
Berkeley, CA 94709
ingram@solar Millennium.com

APPLICANT'S CONSULTANT

Carl Lindner
AECOM Project Manager
1220 Avenida Acaso
Camarillo, CA 93012
carl.lindner@aecom.com

Ram Ambatipudi
Chevron Energy Solutions
150 E. Colorado Blvd., Ste 360
Pasadena, CA 91105
rambatipudi@chevron.com

CO-COUNSEL FOR APPLICANT

Scott Galati, Esq.
Galati/Blek, LLP
455 Capitol Mall, Suite 350
Sacramento, CA 95814
sgalati@qb-llp.com

Peter Weiner
Matthew Sanders
Paul, Hastings, Janofsky & Walker LLP
55 2nd Street, Suite 2400-3441
San Francisco, CA 94105
peterweiner@paulhastings.com
matthewsanders@paulhastings.com

INTERESTED AGENCIES

Holly L. Roberts, Project Manager
Bureau of Land Management
Palm Springs-South Coast Field Office
1201 Bird Center Drive Palm Springs,
CA 92262
CAPSSolarPalen@blm.gov

California ISO
e-recipient@caiso.com

INTERVENORS

California Unions for Reliable Energy
(CURE)
Tanya A. Gulesserian,
Marc D. Joseph
Adams Broadwell Joseph & Cardozo
601 Gateway Boulevard, Suite 1000
South San Francisco, CA 94080
tgulesserian@adamsbroadwell.com

ENERGY COMMISSION

Karen Douglas
Chair and Presiding Member
kldougla@energy.state.ca.us

Robert Weisenmiller
Commissioner and Associate
Member
rweisenm@energy.state.ca.us

Raoul Renaud
Hearing Officer
rrenaud@energy.state.ca.us

Alan Solomon
Project Manager
asolomon@energy.state.ca.us

Lisa DeCarlo
Staff Counsel
ldecarlo@energy.state.ca.us

Public Adviser's Office
publicadviser@energy.state.ca.us

DECLARATION OF SERVICE

I, Carl Lindner, declare that on June 16, 2010, I served and filed copies of the attached:

Computational Fluid Dynamics Modeling of an Air Cooled Condenser in a Convectively Unstable Boundary Layer

The original document, filed with the Docket Unit, is accompanied by a copy of the most recent Proof of Service list, located on the web page for this project at:

[\[http://www.energy.ca.gov/sitingcases/solar_millennium_blythe\]](http://www.energy.ca.gov/sitingcases/solar_millennium_blythe).

The document has been sent to the other parties in this proceeding (as shown on the Proof of Service list) and to the Commission's Docket Unit, in the following manner:

(Check all that Apply)

For service to all other parties:

sent electronically to all email addresses on the Proof of Service list;

by personal delivery or by overnight delivery service or depositing in the United States mail at Camarillo, California with postage or fees thereon fully prepaid and addressed as provided on the Proof of Service list above to those addresses **NOT** marked "email preferred."

AND

For filing with the Energy Commission:

sending an original paper copy and one electronic copy, mailed and emailed respectively, to the address below (preferred method);

OR

depositing in the mail an original and 12 paper copies, along with 13 CDs, as follows:

CALIFORNIA ENERGY COMMISSION

Attn: Docket No. 09-AFC-6
1516 Ninth Street, MS-4
Sacramento, CA 95814-5512

docket@energy.state.ca.us

I declare under penalty of perjury that the foregoing is true and correct.